land

MDPI

*Article*

# Pedestrian Dynamic Thermal Comfort Analysis to Optimize Using Trees in Various Urban Morphologies: A Case Study of Cairo City

**Ahmed Yasser Abdelmejeed [1,2,*] and Dietwald Gruehn [1]**

[1] Research Group Landscape Ecology and Landscape Planning (LLP), Department of Spatial Planning, TU Dortmund University, 44227 Dortmund, Germany; dietwald.gruehn@tu-dortmund.de
[2] Faculty of Urban and Regional Planning, Cairo University, Cairo 11562, Egypt
* Correspondence: ahmed.abdelmejeed@tu-dortmund.de

**Abstract:** Considering the impacts of climate change on the goal of obtaining sustainable and healthier cities, this research aimed to analyze and assess the impact of different urban forms with different trees densities on the dynamic physiological equivalent temperature (DPET) for pedestrians while walking further than the average walking distance (750 m) using ENVI-met. This study included five different areas within Greater Cairo, which is suffering from extreme heat stress. The selected study areas had lots of urban variety in terms of the canyons' aspect ratios, orientations, urban form, green areas, mixed uses, and tree densities. Two tree scenarios were analyzed: the current tree density situation and a scenario where the tree density of each study area was increased to its capacity. The results proved that the DPET had different values than the steady physiological equivalent temperature (SPET) at each point within the walking routes. However, the DPET was closely related to changes in the SPET. Keeping the SPET lower or higher for a long time reduced or increased the DPET, and frequent changes (up and down) in the SPET kept the DPET stable. Changes between DPET values were driven more by the microclimate conditions of a space or canyon than the conditions of the overall area, and controlling the microclimate conditions of a whole urban canyon controlled the DPET. Changes in the DPET could reach as high as 10 °C between different walking routes, and increasing the tree density could help lower the DPET by as much as 6 °C in some cases.

**Keywords:** urban heat island (UHI); outdoor thermal comfort; urban trees; urban shading; dynamic thermal comfort; static/steady thermal comfort; ENVI-met greenery simulation; urban cooling strategies

check for updates

**Citation:** Abdelmejeed, A.Y.; Gruehn, D. Pedestrian Dynamic Thermal Comfort Analysis to Optimize Using Trees in Various Urban Morphologies: A Case Study of Cairo City. *Land* **2024**, *13*, 1489. https://doi.org/10.3390/land13091489

Academic Editors: Yongze Song and Zihao Zheng

Received: 7 August 2024
Revised: 11 September 2024
Accepted: 12 September 2024
Published: 14 September 2024

**Copyright:** © 2024 by the authors. Licensee MDPI, Basel, Switzerland. This article is an open access article distributed under the terms and conditions of the Creative Commons Attribution (CC BY) license (https://creativecommons.org/licenses/by/4.0/).

## 1. Introduction

Developing healthy cities and communities is necessary, especially in light of the impacts of climate change. A healthy and sustainable urban environment consists of a series of pedestrian walkways for commuting, exercising, and leisure use [1]. Walking is considered the most widespread mode of transport [2] as it is a crucial link between the other modes, and pedestrian activity helps to fulfill recreational requirements [3]. People moving between interconnected spaces perform non-sedentary activities, enhancing sustainability and well-being. However, adverse weather conditions may create uncomfortable thermal sensations that change or ruin the experiences of people walking outdoors [4]. The thermal conditions of linear walking paths, which affect a person's thermal comfort, will inherently influence people's usage probability [1]. Therefore, enhancing pedestrian thermal comfort and microclimate conditions is crucial.

### 1.1. Thermal Comfort

Thermal comfort is defined in ASHRAE 55 [5] as a condition of the mind where satisfaction with the thermal environment is expressed. Maintaining a body temperature

at approximately 36–37 °C is essential for regulating the body's metabolic rate and organ function [6]. Hyperthermia and hypothermia both take a toll on physical and psychological health [7].

The PET (physiological equivalent temperature) was designed to measure environmental and personal parameters, including air temperature, air humidity, air velocity, the mean radiant temperature (Tmrt), clothing insulation, and the level of activity, to predict thermal comfort [8]. Thermal comfort can be studied and analyzed in two main ways. The first, which has been used in many studies, is to analyze thermal comfort at a fixed point, which is assumed to be close to steady, based on individuals' instantaneous subjective thermal sensation or comfort while sitting or standing [1]. In this research, this is named the steady PET (SPET). The other way to measure the PET is more dynamic as it focuses on the thermal comfort of pedestrians while walking. In this way, the outdoor thermal environment and the human physiological response are both important determinants of thermal comfort during the dynamic process of walking [1]. In this research, this is named the dynamic PET (DPET).

### *1.2. Difference between DPET and SPET*

Pedestrians receive various continuous changes in microclimate conditions while walking outdoors. Their actual sensations vary over the entire length of a route, sometimes showing significant changes in thermal perception. Subtle environmental changes can affect skin temperature receptors. Physiological responses and thermal experience history are important factors for pedestrian thermal sensation. The steady thermal comfort model is only applicable to people who stay in outdoor environments for 10 to 30 min [1,9,10].

Thermal comfort indices and findings from early studies, which were obtained in thermally homogenous and stable environments, are insufficient to explain constructively the transient thermal perceptions of pedestrians, who are exposed to constantly changing environmental conditions due to urban geometry [11,12]. Traditional environments with steady thermal comfort sometimes cannot meet people's requirements, and dynamic thermal comfort is considered better. In an outdoor summer study, participants walked along a specific route that passed through diverse urban textures, exposing them to a variety of thermal environments that routine fixed-point observations could not capture [13]. In another study, simulation experiments were conducted in a climate chamber. Airport passengers experienced three different durations of walking (5 min, 10 min, and 15 min) at 26 °C and subsequently transitioned to sedentary conditions at three different operative temperatures (23 °C, 26 °C, and 29 °C). By analyzing the variations in subjective perception and physiological parameters, it was concluded that the thermal equilibrium requires 17–21 min to recover to steady-state sedentary levels after walking [14]. Also, a study determined that the SPET has a big impact on the DPET. For example, the steady thermal conditions at the start of a walk significantly impacted the DPET. For a person coming out of a shaded area of a sidewalk and entering a 200 m long sunny segment, after 180 s, his actual skin temperature was approaching the value simulated by a steady-state thermal comfort model, and his core temperature was lower than the simulated value. It was further suggested that around 30 min were required for a person to reach a steady state after leaving a room with thermal comfort to enter hot conditions [15].

### *1.3. DPET Parameters*

Dynamic thermal comfort is affected by the same thermal comfort parameters. Efforts to achieve comfort during walking need to consider both temporal and spatial variations, as well as opportunities for adaptation [4]. Pedestrians are usually alternately exposed to cool-biased and warm-biased environments during outdoor activities, such as when being exposed to indoor and outdoor places or moving through areas with sunlight and shade on the street [9]. Step changes in microclimate environments occur during the above alternate exposures to cool-biased and warm-biased environments, which are mainly characterized by mixed changes in radiation, wind speed, and air temperature. Additionally, these

step changes happen at various frequencies due to the movement speed, the needs of activities, and environmental designs. Essentially, people are in highly dynamic and complex environments when conducting outdoor activities and are speculated to produce thermal responses different from those in relatively steady environments [9]. A previous study found that wind and solar radiation were the main factors attributed to variations in outdoor thermal comfort in any given period [4]. During walking, disturbances due to wind velocity had a significant effect on thermal sensation, which was reflected in an enhancement of convective heat transfer on the skin surface [16]. Another study was carried out from May to July at a university campus in Hong Kong with subtropical weather conditions. The results showed that subjective thermal perceptions varied with alternating exposure to sunlight and shade at different frequencies. With a higher alternating frequency, there was reduced thermal dissatisfaction with hot summer days and a lower comfort requirement for shade [9]. Also, a very important factor that impacted the DPET was the metabolic rate. Full consideration should be given to variations in this variable. Typically, it takes 3–5 min to reach a new metabolic level when walking indoors, whereas it takes 9–11 min in a transition space. In the meantime, the metabolic rate returns to a normal sedentary level 3–5 min after walking ceases in both indoor and transition spaces [16].

### *1.4. Urban Geometry Effect*

Improving urban geometric design is necessary to mitigate thermal discomfort and create better pedestrian environments, especially in high-density cities [12]. Urban morphology, the sky view factor (SVF), and shading are the major factors that have significant roles in enhancing microclimate conditions [17,18]. The shadows cast by buildings help reduce the pedestrian radiant load and, consequently, improve thermal comfort [19–21]. Openness is a predominant factor that influences pedestrians' thermal comfort, and pedestrians have also been shown to feel more comfortable when moving from sunlit places to shaded places [12]. A study showed that greater cooling of road microclimates occurs on roads with low SVFs [22]. The street canyon orientation and aspect ratio have significant influences on urban microclimates and directly impact street-level thermal comfort [23,24], as the aspect ratio controls the amount of shadow and the orientation affects the wind speed based on the wind direction. Optimizing shadows and wind speeds using the aspect ratio and orientation will lead to significant enhancements for both the SPET [21,25–27] and DPET [4,9].

### *1.5. Urban Trees*

Urban greenery and biotopes represent discernible cool spots along walking paths [13]. They can reduce the effects of the surrounding building mass and help to create a low-SVF environment that is cooler during both daytime and nighttime [28]. Studies have demonstrated that walking in forest environments diminishes blood pressure, skin conductivity, muscle tension, pulse rate, cortisol levels, and sympathetic nerve activity and enhances parasympathetic activity (the components of heart rate variability) [29,30]. Also, a roadside landscape may have a proportionally greater impact on urban dwellers due to the limited availability of green spaces in cities. Urban roadside trees can improve urban dwellers' feelings and can make a city cooler [22]. According to this study, we can infer that a short walk along an urban road surrounded by trees is a simple, attainable, and effective method of improving the quality of life and well-being of urban dwellers [22]. As a combined impact, it has been demonstrated that urban morphology and vegetation shading affect solar radiation storage during the day in summer, especially for low-rise buildings [21,28,31]. Also, trees' thermal performance is significant for different orientations of canyons, especially the eastern–western orientation [21,32,33].

### *1.6. Research Gap and Target*

This research aimed to study the impacts of different urban forms and different densities of urban trees on pedestrian thermal comfort while walking from a dynamic

thermal comfort perspective under the same climate conditions (same climate data input), as pedestrian dynamic thermal comfort for people who are moving at a certain speed and not stopping at any one place for a long period is not well studied [1]. This study sought to understand the impacts of different urban forms (different aspect ratios, orientations, and tree densities) on pedestrian dynamic thermal comfort while walking between different destinations within different urban areas.

This knowledge helped clarify how different urban forms perform thermally and how many trees are needed to enhance the thermal performance of each urban form to improve the microclimate conditions and the dynamic thermal comfort of pedestrians while walking.

## 2. Materials and Methods

To assess dynamic thermal comfort for different urban forms and tree densities, this study was conducted on various walking routes in different urban areas with different tree densities. It tested different urban forms (with different aspect ratios and orientations) and different tree canopy covering densities by measuring the DPET on each route in each study area under different tree scenarios using the microclimate simulation software ENVI-met V5.6.1 and its dynamic thermal comfort analysis capability, which was released in June 2023 [34]. This study was carried out through two main steps, as shown in Figure 1.

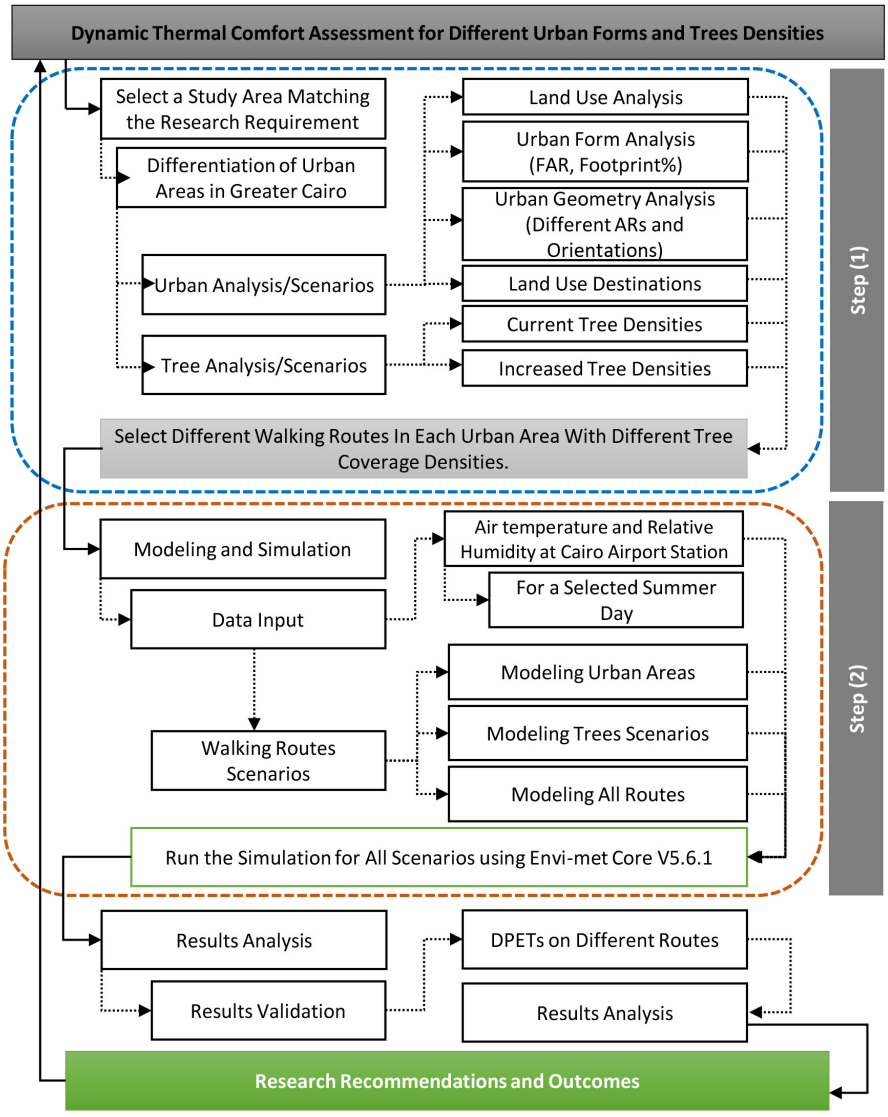



**Figure 1.** Research methodology.

In step (1), a city that suffers from very high levels of heat stress and high solar radiation with variety between different areas was selected to obtain better results for different urban cases before and after applying trees scenarios. Also, the study areas included land use destinations that people would be moving between and access to public transportation modes. In the same step, a complete urban geometry and tree analysis was applied to understand how the existing urban geometries and proposed tree variations impacted the results. In step (2), scenarios were simulated after completing all meteorological inputs for the city and modeling different scenarios and routes. Then, the simulation results were validated and analyzed to understand the differences in each urban area with different tree coverage densities.

### *2.1. Step (1): Study Area Selection and Analysis*

The city selected as the study area was the metropolitan area of Cairo, which suffers from heat stress as the city is located in a dry desert in a subtropical climatic region and has a warm summer climate based on the Köppen–Geiger climate classification [35]. During summer (June to August), it is hot and dry with an average temperature of around 28 °C [36,37] and a maximum average temperature of around 35 °C. The urban heat island effect (UHI) appears clearly in the city of Cairo. In previous studies, it was found that the UHI ranges from 0.5 to 3.5 °C [38]. The maximum observed difference was 10 °C compared to the surrounding rural or desert areas [36,39,40]. Cairo City is very large and has lots of urban variety as the city has grown over many decades and is still evolving and growing rapidly [41,42]. The selection of Cairo City allowed different urban areas with different urban forms, morphologies, and tree scenarios to be studied, which suited the purpose of this study. The selection of the study areas within Cairo was carried out carefully to ensure that there were appropriate differences between them in terms of urban forms and morphologies as this helped clarify the different intensities of the impacts on pedestrians while walking, especially the impacts of trees in the respective situations and when the tree densities were increased.

#### 2.1.1. Urban Analysis of Study Areas

As shown in Figure 2, five study areas were selected (Bulaq Ad Daqrur (known as Bulaq), Khedival Cairo (known as Downtown), Mohandisen, New Cairo, and Mivida). They were characterized by different urban morphologies, and the tree density varied between them. Additionally, the locations of the selected study areas were different, as three of them (Bulaq, Downtown, and Mohandisen) were very close to the center of Cairo (within a 4 to 5 Km range) and two areas (New Cairo and Mivida) were suburban areas (around 17–29 Km away from the city center). Table 1 shows the local climate zones and the main urban characteristics of each study area. As shown in Figure 3, the selected study areas had similar sizes, as they varied between 18 and 22.9 hectares, and changes in the solid-to-void ratio (footprint of buildings divided by the site area) were obvious. It varied from 75% solid in Bulaq to 61% and 59% in Mohandisen and Downtown to a low solid percentage of 29% in New Cairo and a very low solid percentage of 13% in Mivida. Also, the green areas were different, as they were 0% in Bulaq and Khedival Cairo, with a very limited green area of 3% in Mohandisen and good amounts of greenery of 12% in New Cairo and 23% in Mivida.

The floor area ratio (FAR, the total built-up area divided by the site area) changed between the different areas as a reflection of the footprint percentage and building heights. It ranged from a high of 5.2 in Bulaq to moderate values of 4.58 and 4.31 in Downtown and Mohandisen to a low value of 1.15 in New Cairo and a very low value of 0.39 in Mivida. Figure 4 shows the variation in building heights and the urban destinations (including public transportation) in each area. The maximum building height was in Mohandisen, where most of the buildings were in the range of 28 m to 40 m (9 to 13 floors). Medium building heights in the range of 22 m to 27 m (7 to 9 floors) were observed in Bulaq and Downtown. The lowest buildings, in the range of 9 m to 12 m (3 to 4 floors), were in New

Cairo and Mivida. A greater number of public transportation facilities were located in Downtown, which had a metro station and a bus stop. Two bus stops were located in Bulaq and Mohandisen, and one bus stop was located in New Cairo. No public transportation facilities were located in Mivida, as it is a gated community that is more car-centric, and the walking circulation depends on internal movements between the community amenities. The different urban analyses showed that there were too many differences between the study areas and that the selected study areas had significant variety. This was reflected in the results, helped to cover more cases, and provided a better understanding of the impact of each change.

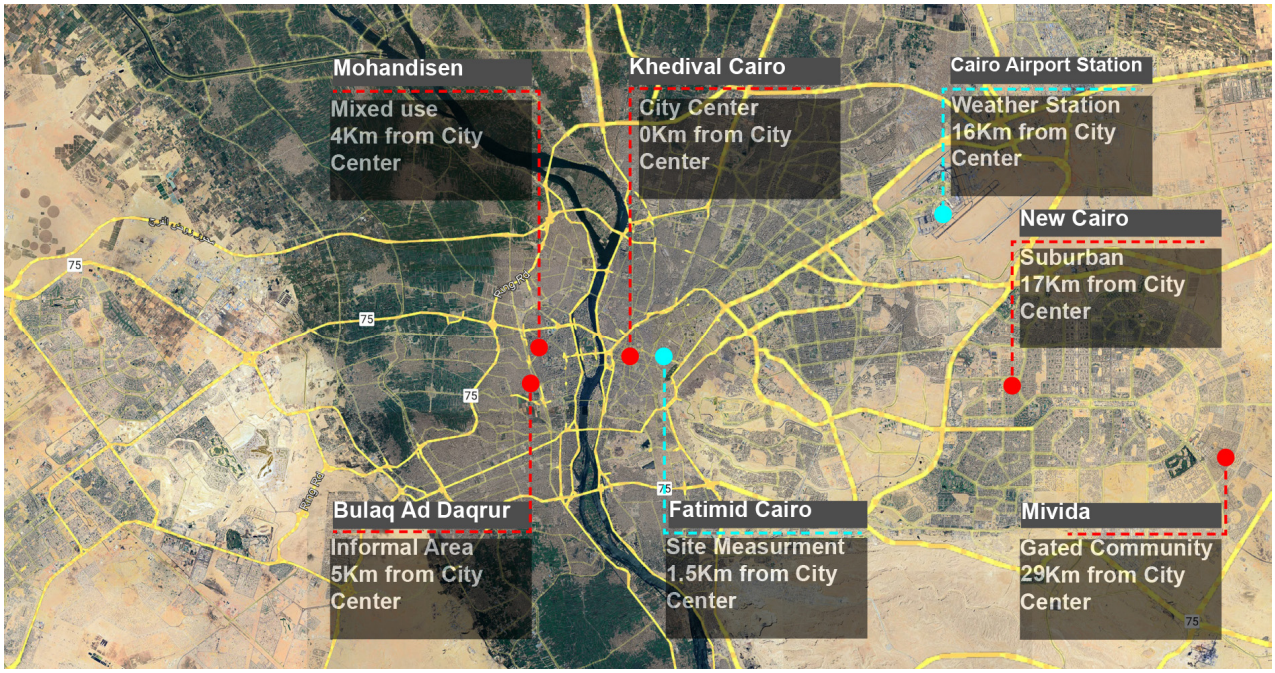



**Figure 2.** Selected study areas, Cairo weather station, and site measurement location.

**Table 1.** The climate zones and characteristics of the urban areas.

| Study Area | Bulaq Ad Daqrur (Bulaq) | Khedival Cairo (Downtown) | Mohandisen | New Cairo | Mivida |
|---|---|---|---|---|---|
| Local Climate Zone (LCZ) * | LCZ2 Compacted midrise | LCZ2 Compacted midrise | LCZ1 Compacted high rise. | LCZ5 Open midrise | LCZ6 Open low rise |
| Urban Classification | Informal area | City center | Business center | Suburban community | Gated community |
| Aspect ratio | Deep | Moderate | Moderate | Open canyons | Shallow canyons |
| Mixed uses and car/transit orientation | Low mixed uses, transit-oriented | High mixed uses, transit-oriented | High mixed uses, transit- and car-oriented | Low mixed uses, car-oriented | No mixed uses, car-oriented |
| Density | Very high | Moderate | Moderate | Low | Very low |

* Local climate zones (LCZs) were classified as explained in [43,44].

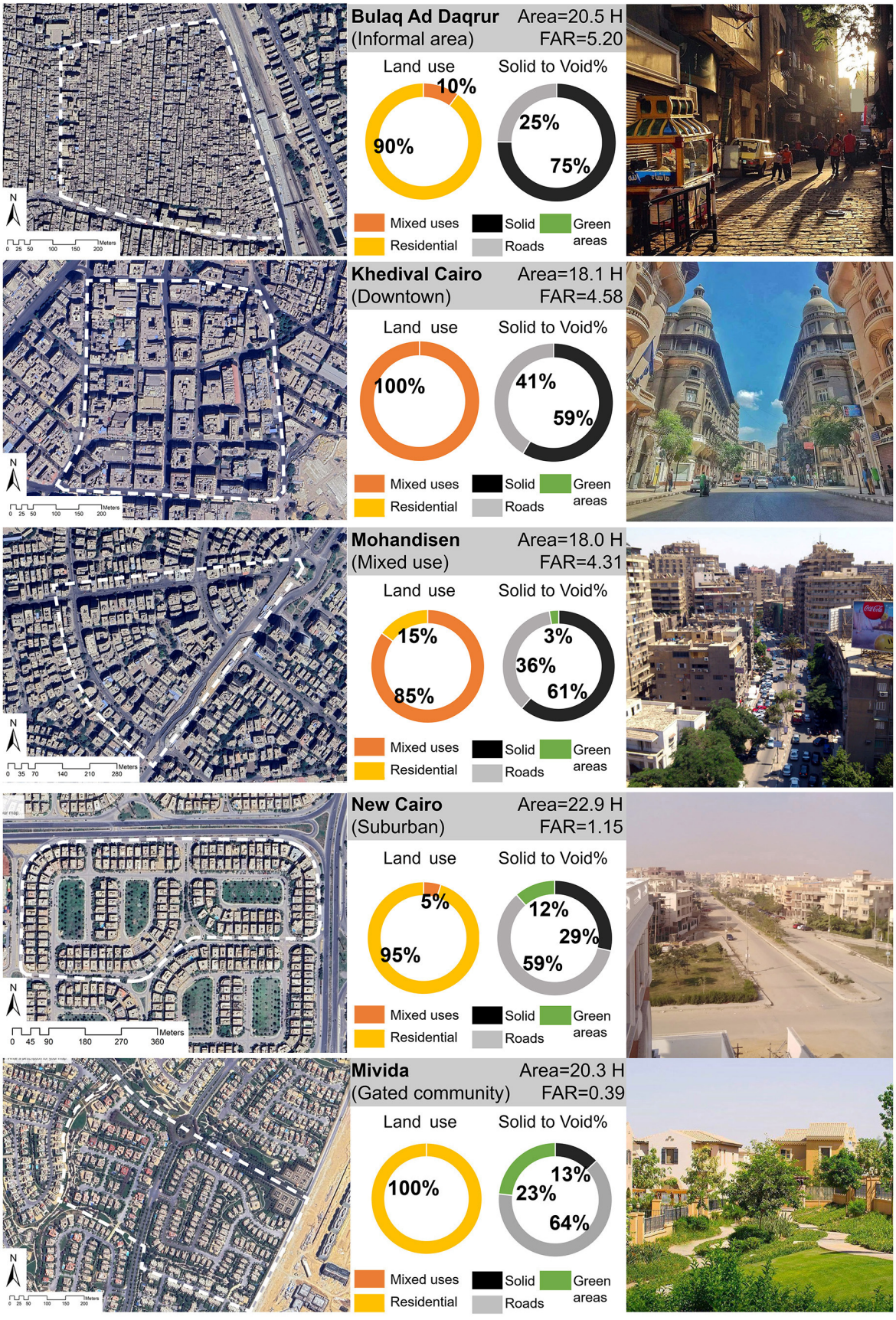



**Figure 3.** Urban analysis of study areas.




**Figure 4.** Study areas (building heights, street names, and main urban features).

2.1.2. Tree Scenarios

The study areas not only had various urban morphologies and changes; they also had good variety with respect to tree density. As shown in Figure 5, the existing tree coverage percentages varied significantly between the study areas. They were very low (2.1%) in Bulaq and reached 6.2% in Downtown and 7.8% in Mohandisen. These percentages were very low, indicating that there were only a few open spaces in these three study areas. On the contrary, the percentages of tree coverage for open spaces were moderate in New Cairo (9.4%) and high in Mivida (13%), indicating that open spaces occurred more frequently in these study areas.

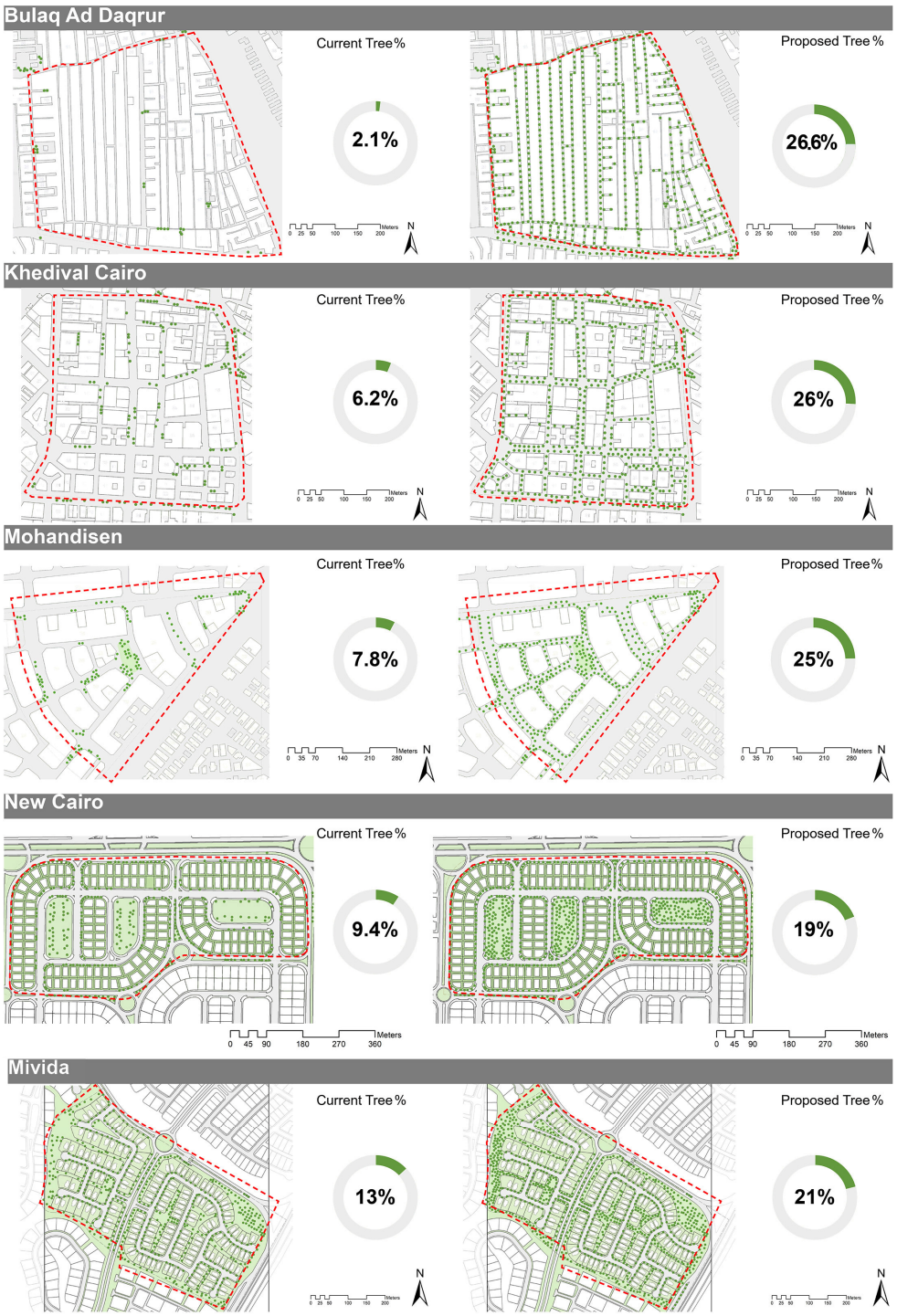



**Figure 5.** Current and proposed tree densities for each study area.

To investigate the impacts of trees in each area, this study not only tested the current tree situations but also scenarios with increasing tree densities. The proposed increases in tree densities are indicated on the right side of Figure 5. They were tested to understand the impacts of increases in trees in each urban morphology to better understand how this would impact the DPET of people walking in each study area. Tree density was increased to achieve a good distribution of trees and good tree spacing on roads and in parks. Adding trees led to different tree coverage percentages in each study area, as shown in Figure 5. In Bulaq, increasing the number of trees helped to increase the tree coverage percentage of the open spaces from 2.1% to 26.6%, which was significant because of the limited open space areas. In Downtown, it was increased from 6.2% to 26%, which was also a significant increase, as the open space areas were bigger than in Bulaq. A similar increase from 7.8% to 25% occurred in Mohandisen, as the open space areas were similar to those in Downtown. In New Cairo and Mivida, the tree coverage percentages were similar, with limited increases from 9.4% to 19% in New Cairo and from 13% to 21% in Mivida. However, many more trees were added than in the other areas. Because of the bigger open spaces, the density increased at lower rates compared to the other areas.

Testing these tree scenarios and the impacts of low and high densities of trees in each study area provided a comprehensive understanding of how trees perform in each urban morphology/local climate zone and helped clarify which tree density is required for each urban morphology. This will lead to optimization of the use of trees in each urban area, as shown in previous studies [21,45].

#### 2.1.3. Walking Routes

As this study focused on the dynamic thermal comfort of pedestrians, the selection of the walking routes in each of the different scenarios was very important. As the study results focused on the DPETs of the routes and locations, the design of each route (in relation to different aspect ratios, orientations, and trees densities) was the focus of this study. Therefore, in each study area, two routes were provided to ensure that the majority of the area was covered by walking routes. The walking routes did not overlap, and each route connected the main urban features in each study area, such as the transportation stations, retail areas, amenities, parks, etc. [1]. Figure 6 shows the proposed routes in each study area. They were designed to pass the different elements in each area. In Bulaq, the routes passed different aspect ratios and orientations. Route (A) started at the bus stop, moved through the wide eastern canyon (H:W 1:0.75), then moved through the narrow northern canyon (H:W 3:1) to reach a residential destination. Route (B) started at the second bus stop, moved through the narrow eastern canyon (H:W 3:1), then moved to a second residential destination through the narrow northern canyon (H:W 1:2.5). Similarly, in Downtown, route (A) started at the metro station, moved through a wide eastern canyon (H:W 1:1.25), through a moderate northern canyon (H:W 1:1), then through a moderate eastern canyon (H:W 1:1.25) to reach a retail destination. Route (B) started at the urban park next to the bus stop, moved through a moderate eastern canyon (H:W 1:1), a moderate northern canyon (H:W 1:1.3), then a moderate eastern canyon (H:W 1:1.5) to reach the coffee shop area.

In Mohandisen, route (A) started at the bus stop, moved through a moderate eastern canyon (H:W 1:1) and a northern canyon, passing by an urban park with dense vegetation, and moved through an eastern canyon (H:W 1:1) to reach a residential destination. Route (B) started at the same point at the bus station, moved through a shallow northeastern canyon (H:W 1:3.5) for most of the trip, then through a moderate northwestern canyon (H:W 1:1). In New Cairo and Mivida, the routes passed different urban contexts, including very shallow roads (H:W 1:3) and urban parks, as shown in Figure 6.

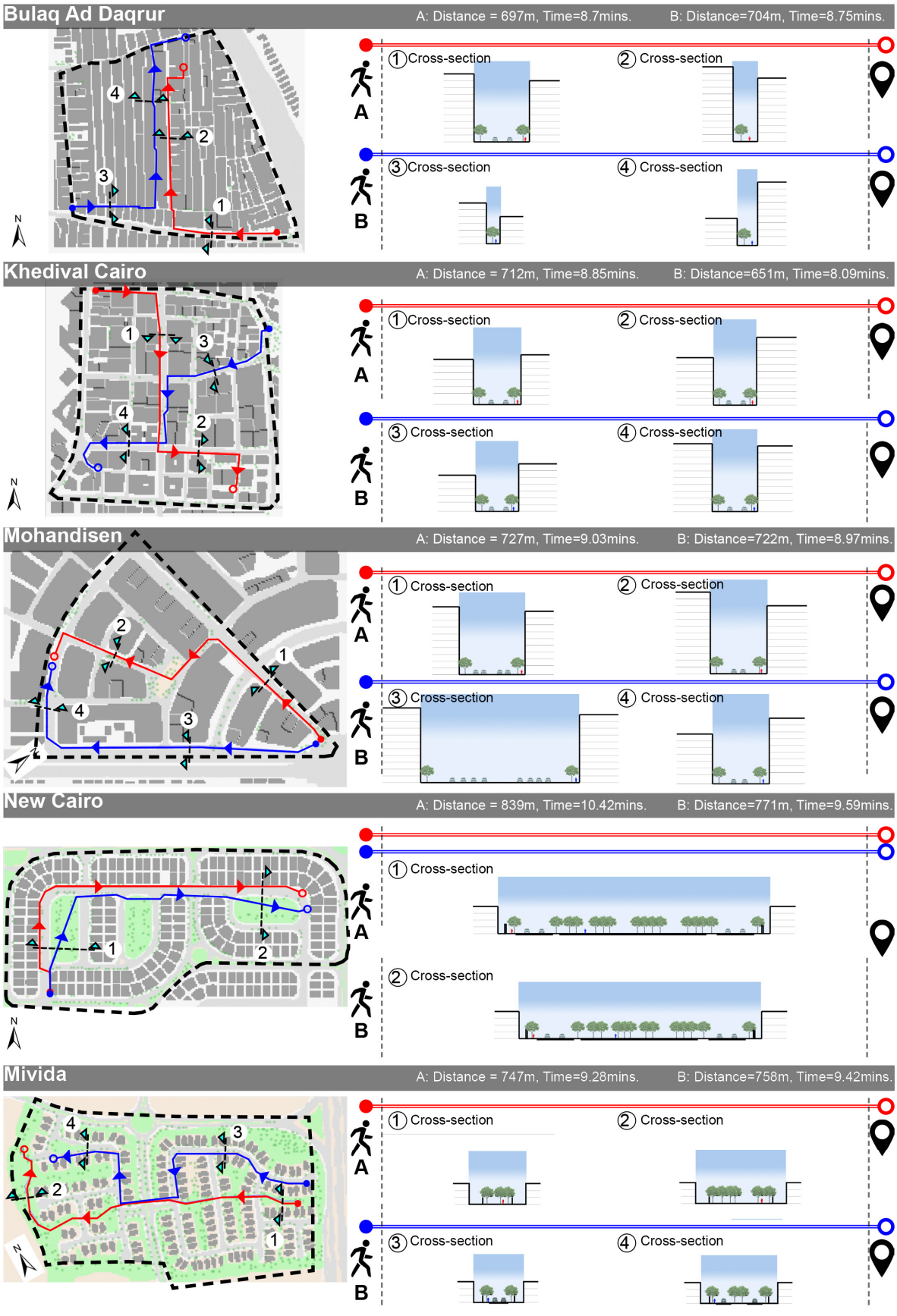



**Figure 6.** Alignment of pedestrian routes and cross-sections of different segments in each study area.

The routes were designed to be as long as possible as this study was more focused on long-distance pedestrian routes, which represent the main research gap [1]. Therefore, all designed routes were longer than the walking distance range, which is 500 m [4]. The route lengths in Bulaq, Downtown, Mohandisen, New Cairo, and Mivida were A = 697 m and B = 704 m, A = 712 m and B = 651 m, A = 727 m and B = 722 m, A = 839 m and B = 771 m, and A = 747 m and B = 758 m.

The different routes in each study area were tested under the two tree scenarios (the current tree coverage and the proposed tree coverage). This study was applied to 20 different routes with different morphologies and urban tree densities. This variation in the tested routes provided more detailed and variable results, which enriched the research findings.

### *2.2. Step (2): Data Input, Model Set-Up, and Measuring Points*

The software used to run the simulations for the different cases in each study area under different tree scenarios was ENVI-met V5.6.1, Winter 2023. All of the information required for the model was provided, representing existing urban configurations (material and soil) of common materials in Cairo, as well as meteorological data.

#### 2.2.1. Model Set-Up and Geometry

The model's location was 30.02 latitude and 31.22 longitude. This was obtained from the ENVI-met V5.6.1, Winter 2023 database by selecting the location of Greater Cairo in the ENVI-met application "Spaces". As shown in Table 2, all models were created using the following model geometry: materials, soil, and trees.

**Table 2.** Model set-up and geometry for each study area.

| Model Information | Bulaq | Downtown | Mohandisen | New Cairo | Mivida |
|---|---|---|---|---|---|
| Area size (grids) | X = 205, Y = 186, Z = 30 | X = 167, Y = 170, Z = 30 | X = 233, Y = 192, Z = 27 | X = 259, Y = 121, Z = 12 | X = 239, Y = 128, Z = 8 |
| Grid resolution (m) | X = 3, Y = 3, Z = 3 | X = 3, Y = 3, Z = 3 | X = 3, Y = 3, Z = 3 | X = 3, Y = 3, Z = 3 | X = 3, Y = 3, Z = 3 |
| Orientation | 0 | 0 | −50 | 0 | 32 |
| Split lower grid box into 5 sub-cells | Yes | | | | |
| Telescoping applied | Not applied, as the maximum building height was not very high | | | | |
| Maximum model height * | 90 m | 90 m | 81 m | 36 m | 24 m |
| Nesting grids ** | 5 grids, sandy soil | | | | |
| DEM | Not applied, as the site was flat | | | | |
| Soil | Asphalt for roads, concrete for sidewalks and under buildings, loamy soil for green areas. | | | | |
| Building materials | Default wall—moderate insulation | | | | |
| Tree model and size | Latin name: *Acer platanoides* *** Height = 15 m; crown width = 7 m | | | | |

* The model's height was more than double the height of the tallest building, as recommended by the software [34]. ** Nesting grids were added, in addition to five cells from the boundary sides of the model being kept empty, as recommended by the software developers [34]. *** *Acer platanoides* was selected from the ENVI-met database as it met the required criteria of having a large canopy, a high LAD, and a good canopy height, matching the recommendations in [46–49]. Different trees would have different impacts and performances [50]. This study used one recommended tree characteristic to measure the impacts of other elements such as the aspect ratio, orientation, canyon side, and tree density.

#### 2.2.2. Simulation Configuration

The simulation was configured for a representative summer day (i.e., the hottest day of July: 2 July 2023) as the hottest days in summer occur between June and July based on an analysis of 30 years of data from the Cairo Airport station [51]. The same air temperature,

relative humidity, and wind speed were added to ENVI-met for each hour of the simulated day, and climate data were imported from the Cairo Airport weather station for all study areas as the main focus is the analyze the impact of the urban form and trees densities under the same climate conditions. Its location is shown in Figure 2 [52,53]. The starting time of the simulation was 1:00 a.m., and the total duration was 24 h. ENVI-met simple forcing was used for the metrological data.

#### 2.2.3. Simulation Outputs

Output data were extracted using the ENVI-met ''Bio-met'' to calculate the DPET and SPET values of each route in each study area under the different tree scenarios. The results were exported for five different hours during daytime from sunrise until sunset. The chosen hours were selected to cover the different times when people perform activities and move between different destinations in each urban area. Table 3 shows the selected hours and the trips expected at each hour. The dynamic thermal comfort (DPET), steady thermal comfort (SPET), dynamic skin temperature (T Skin), and average core temperature were exported for each route in each study area for both tree scenarios for the five selected hours (9:00, 11:00, 13:00, 15:00, and 17:00). These hours not only covered the whole daytime but also covered the majority of the pedestrian trips during daytime.

**Table 3.** Selected hours and trips expected at each hour.

| **Hour** | **9:00 a.m.** | **11:00 a.m.** | **13:00 p.m.** | **15:00 p.m.** | **17:00 p.m.** |
|---|---|---|---|---|---|
| Activity (1) | Trip to work | Trip to park | Work break | Leaving work | Leaving work late |
| Activity (2) | Trip from school | | Nursery school closing | Leaving school | Trip to park |
| Activity (3) | Trip to park | | | Late break | Shopping trip |

Table 4 below shows the pedestrian data and the thermal conditions of the starting point of each route as applied in ENVI-met (Biomet). These conditions were applied to all routes for each hour considering the start of a walk with static thermal conditions, as explained in Table 4. These static thermal conditions were exported from the Downtown study area and unified for all other study areas to maintain the same static thermal comfort conditions at the starting points.

**Table 4.** Pedestrian data and the initial climate conditions at each hour.

| **Pedestrian Data (for All Hours) *** | | | | **Initial Climate Conditions at 9:00 **** | | | |
|---|---|---|---|---|---|---|---|
| Gender | Age | Clothing | Speed | Air temperature (°C) | Wind speed (m/s) | MRT | Spec. Humidity |
| Male | 35 | 0.9 clo *** | 1.34 m/s | 28.7 | 0.46 | 49.04 | 11.11 |
| Initial climate conditions at 11:00 ** | | | | Initial climate conditions at 13:00 ** | | | |
| Air temperature (°C) | Wind speed (m/s) | MRT | Spec. Humidity | Air temperature (°C) | Wind speed (m/s) | MRT | Spec. Humidity |
| 31.6 | 0.45 | 56.37 | 10.84 | 33.5 | 0.44 | 59.35 | 10.71 |
| Initial climate conditions at 15:00 ** | | | | Initial climate conditions at 17:00 ** | | | |
| Air temperature (°C) | Wind speed (m/s) | MRT | Spec. Humidity | Air temperature (°C) | Wind speed (m/s) | MRT | Spec. Humidity |
| 34.1 | 0.44 | 57.63 | 10.22 | 33.3 | 0.43 | 47.46 | 10.38 |

* Default personal data in ENVI-met (category named Michael average). ** The current average Downtown microclimate was used for all. *** The selected value (0.9 clo) represents the default value for clothes insulation, not the summer low value because of the study conditions, as this study mainly focused on daytime trips, which are mainly related to work or school, as explained in Table 3, and need more formal clothes. Also, due to cultural aspects of the people in the study area (people usually wear long sleeves and long trousers), using the default value of 0.9 clo was more suitable for this study.

### 2.3. Results Validation

The results (air temperature and relative humidity, as they were more stable than the mean radiant temperature and wind speed [31,54]) of each study area model were compared with the airport station data and data measured on the same day from another study at the center of Cairo. These site measurements were performed using a mobile weather station at a height of 1.1 m from the ground in an outdoor space on Al Muizz Street on the same day (the 2nd of July) in 2012 [51]. The locations of both the site measurements and the weather station are shown in Figure 2. These data are a limitation of this research. Due to a limited research team, limited funds, and security restrictions, which also affected previous studies in Cairo [21,27], the weather station at Cairo Airport provided input data for all cases and the simulation results were validated via comparison with the weather station data and the site measurements on the same day (2nd of July). It was clear that the results were aligned with the data from the Cairo Airport station and the site measurements. As shown in Figure 7, the air temperature and relative humidity had the same values in all models in relation to the station and site measurements. The changes were very minor, and the charts had the same linear shapes. To ensure that all results had good agreement with the measurements, the root-mean-square error (RMSE) and the degree of agreement (d) were calculated for all model results and both measurements. Tables 5 and 6 show the RMSE and d for air temperature and relative humidity. The RMSE values ranged between 1.3 °C and 1.9 °C for the station-measured air temperature and between 1.0 °C and 1.7 °C for the site measurements. The d values ranged between 0.93 and 0.95 for the station-measured air temperature and between 0.92 and 0.98 for the site measurements. For the relative humidity, the RMSE ranged between 4.4% and 9.8% for the station measurements and between 7.1% and 10.3% for the site measurements. Based on these results and comparisons with similar studies conducted in Cairo City [21,27,45], the simulation results are valid, and the output values represent the current situation in Cairo.

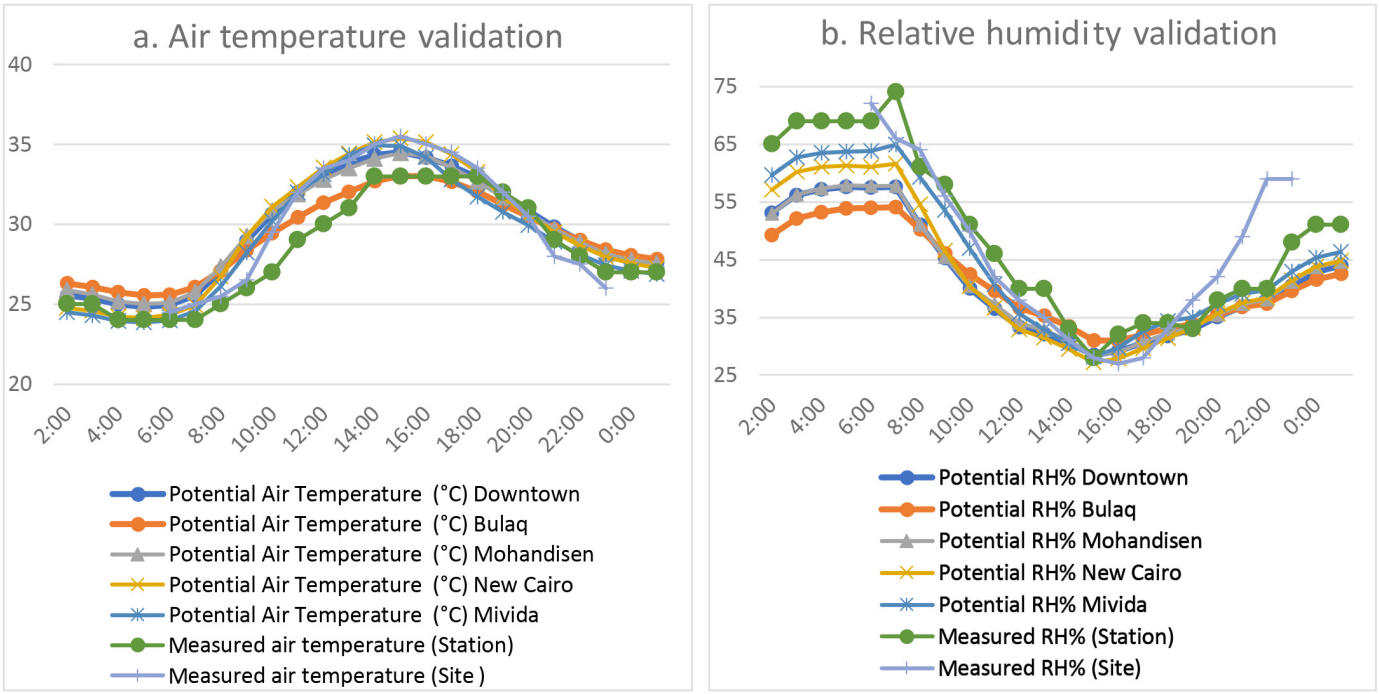



**Figure 7.** Results validation. (**a**) Air temperature. (**b**) Relative humidity.

**Table 5.** RMSE and d for air temperature values.

| | Potential Ta (°C) in Downtown | Potential Ta (°C) in Bulaq | Potential Ta (°C) in Mohandisen | Potential Ta (°C) in New Cairo | Potential Ta (°C) in Mivida |
|---|---|---|---|---|---|
| RMSE (station) | 1.686 | 1.337 | 1.708 | 1.886 | 1.59 |
| RMSE (site) | 1.168 | 1.699 | 1.248 | 1.041 | 0.969 |
| d (station) | 0.937 | 0.949 | 0.932 | 0.931 | 0.948 |
| d (site) | 0.97 | 0.921 | 0.964 | 0.979 | 0.981 |

**Table 6.** RMSE and d for relative humidity values.

| | Potential RH% in Downtown | Potential RH% in Bulaq | Potential RH% in Mohandisen | Potential RH% in New Cairo | Potential RH% in Mivida |
|---|---|---|---|---|---|
| RMSE (station) | 8.634 | 9.83 | 8.364 | 7.014 | 4.418 |
| RMSE (site) | 9.892 | 10.342 | 9.597 | 8.867 | 7.09 |
| d (station) | 0.884 | 0.823 | 0.89 | 0.932 | 0.973 |
| d (site) | 0.824 | 0.775 | 0.833 | 0.873 | 0.92 |

## 3. Results

The results are presented in two stages. In the first stage, the DPET, SPET, T Skin, and avg. TCore are presented for each route in each study area before and after increasing the tree density to understand the impacts of urban morphology, urban trees, and other elements such as the SPET and T Skin on the DPET. In the second stage, the DPET values of each route are compared. In the first case, the DPET of each route is compared to that of the same route after adding trees to understand the trees' impact. The trees' impact is also assessed by analyzing the thermal classification percentages of the walks in both tree scenarios. In the second case, both routes in each study area are compared before and after increasing trees, and in the third case, each route is compared with the other routes in the other study areas. These detailed and varied comparisons provide a complete understanding of how different factors impact dynamic thermal comfort.

### *3.1. SPET at the Starting Point*

To obtain a complete understanding of the static thermal comfort at the starting point of each route in each study area with different tree densities, Figure 8 shows the exact SPET at the starting point of each route. These changes in the SPET values were considered while analyzing the DPET of each route. As shown in Figure 8, the SPET at the starting point of Bulaq route (B) was higher for the hours 11:00, 13:00, and 15:00, and in Mohandisen, the starting point for both routes (A and B) was lower. This was considered in the analysis of the results, as the most important part was how the DPET increased or decreased during the walk. Therefore, if the starting point was too high, the DPET would decrease, and if the starting point was too low, the DPET would increase during the walk. The main impact of the different urban morphologies and tree densities was how the DPET increased or decreased during the walk.

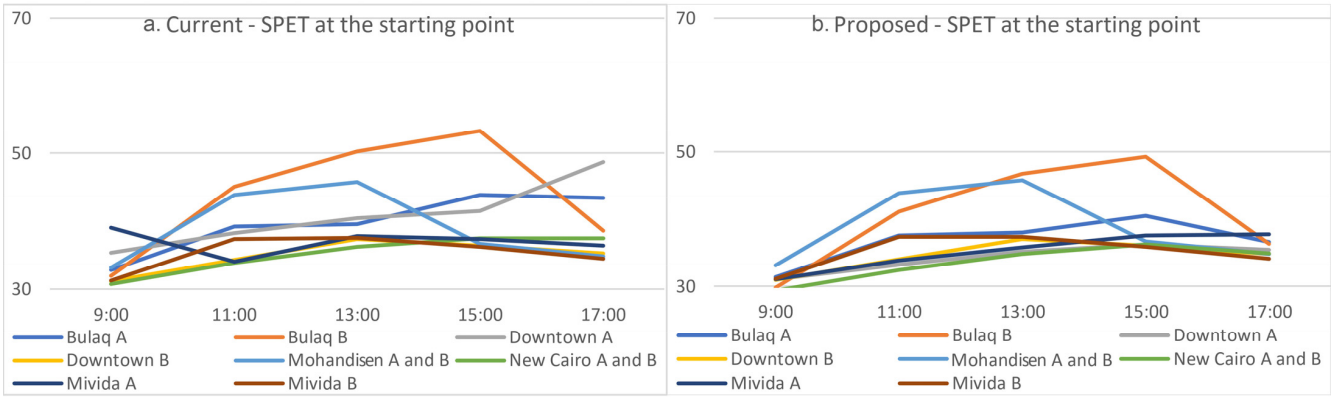



**Figure 8.** The SPET value at the starting point of each walking trip: (**a**) the current tree scenario; (**b**) the proposed tree scenario.

### *3.2. DPET Results*

In Bulaq (Bulaq Ad Daqrur), as shown in Figure 9, at 9:00 both routes (A and B) had almost the same starting DPET value. The difference between them was 1.5 °C. Then, after reaching the end of the eastern route, the difference in the DPET reached 3.5 °C. Once moving on the northern road, both routes' DPET values started to decrease. On route A, the DPET decreased from 36.5 °C to 33 °C, and on route B, the DPET decreased from 34 °C to 31.2 °C at the end. Adding trees helped to reduce the DPET increase during movement on route A to a maximum increase of 1 °C, and route B had almost the same DPET value until the end.

At 11:00, the tight canyons on route B helped, with a total reduction of 5 °C. The opposite result was observed on route A, which had an increase of 4.5 °C on the eastern road over a very short distance. Then, on the northern road, the DPET started to decrease again and almost reached the same value as the starting point. This clearly showed the impact of the wide eastern canyon. Adding more trees led to the same performance for route B but decreased the impact of the eastern canyon on route A, as the increase was 1.5 °C instead of 5 °C.

At 13:00, when the shade from the buildings had almost vanished, the DPET on route A increased by 5 °C on the eastern route, then decreased slightly by 3 °C by the end of the northern road. Route B showed an irregular reduction within 1 °C from the beginning until the end. Increasing the tree density led to significant decreases in the DPET. On routes A and B, the trees helped to reduce the DPET by 3.5 °C and 7 °C.

At 15:00, the tight canyons on route B led to a significant DPET reduction of 6 °C at the end of the walk. On route A, the wide eastern canyon led to an increase of 5 °C. Then, the tight northern canyon helped to reduce this increase to reach the same value as the starting point (40 °C). Adding trees to both canyons helped to avoid this increase in the eastern canyon on route A, as it limited the increase to only 1 °C. On route B, the same regular reduction occurred but with DPET values that were reduced by 8 °C. At both hours (13:00 and 15:00), small fluctuations in the skin temperature occurred on route A due to the impact of the wide eastern road, which had strong heat stress. Then, once on the tight northern route, due to the good urban shading, the skin temperature dropped gradually until the end of the walk.

At 17:00, both roads showed good DPET values, with a slight increase on route B that reached 2 °C, and the values ranged between 36 °C and 40 °C. Adding trees to both routes helped keep the DPET values stable for the whole trips, with DPET values around 35 °C on both routes.

The results for Downtown (Khedival Cairo) are shown in Figure 10. At 9:00, both routes (A and B) showed the same regular increase in DPET, which increased by 5 °C. This increase only took place within the wide eastern canyon. Adding trees helped to reduce the DPET increase by 50%, as it ranged between 2.0 °C and 2.5 °C on both routes. Reducing the DPET values of the whole route to within 30 °C to 33 °C kept them under the skin temperature.

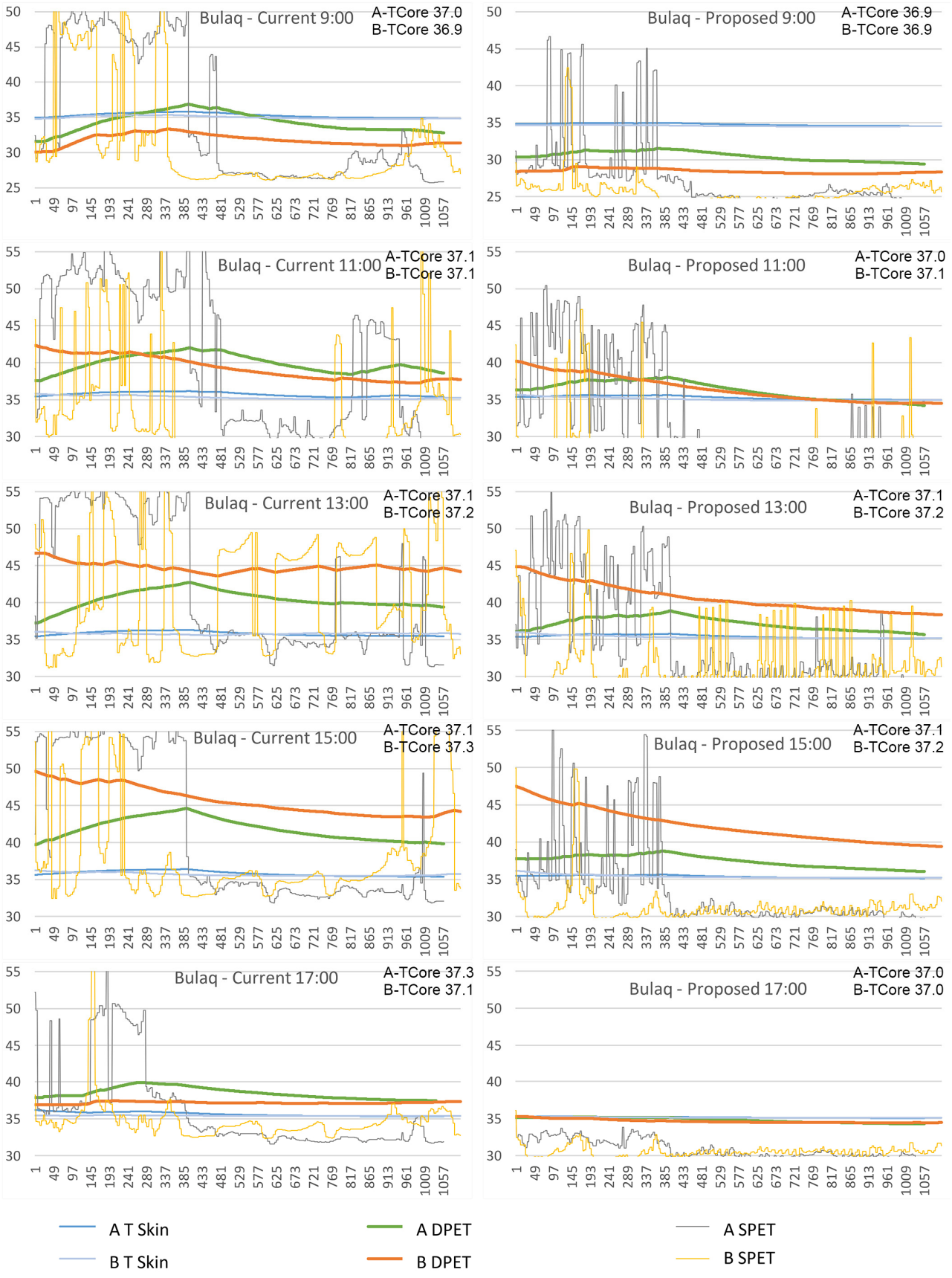



**Figure 9.** DPET, SPET, skin temperature (T Skin), and average core temperature (TCore) results for Bulaq routes (A and B) in both tree scenarios (current and proposed) at Z = 1.5 m. Y axis = °C and X axis = seconds while walking each route.

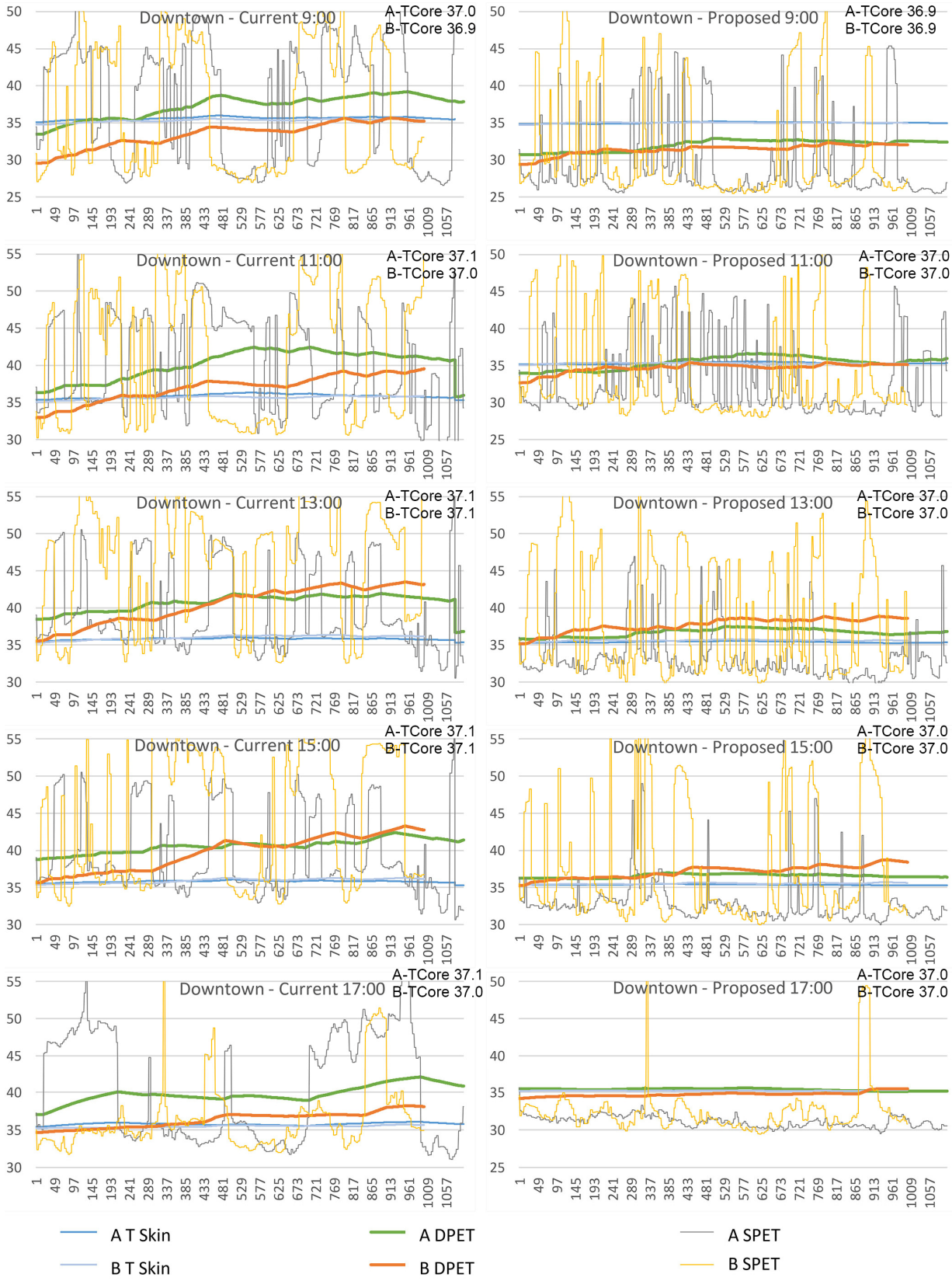



**Figure 10.** DPET, SPET, skin temperature (T Skin), and average core temperature (TCore) results for Downtown routes (A and B) in both tree scenarios (current and proposed) at Z = 1.5 m. Y axis = °C and X axis = seconds while walking each route.

At 11:00, the same regular increase in DPET occurred. It was lower on route A, which started at DPET = 36 °C, reached 42.5 °C, and ended at DPET = 41 °C for an increase of 5 °C. Route B showed a regular increase, especially on the eastern roads, with an increase of 6.5 °C. Increasing the tree density helped to keep the DPET almost stable during the whole walk within the range of 34 °C to 36 °C and in the range of the skin temperature

At 13:00, route A showed a good performance with a 2.5 °C increase. However, on route B, which started at a lower DPET value, the eastern canyons led to a significant increase of 7.5 °C, and the DPET reached 43 °C at the end of the walk. Increasing the tree density helped reduce the values at the starting points for both routes. Route A stayed within the same range until the end of the walk, and the increase on route B was significantly reduced. It only reached 3 °C, which was 60% lower.

At 15:00, a similar performance was observed. A slight increase in the DPET on route A reached 3 °C, which reflected the good cooling performance of the northern road. On route B, the same increase of 7 °C occurred by the end of the walk, with regular increases on the eastern roads and steady DPET values on the northern road. However, route B started with a DPET value that was 3.5 °C lower than that of route A's starting point, and route B ended 1 °C higher than route A. This was because of the impact of the canyon orientation. Increasing the tree density led to similar performances, and both routes maintained good DPET values. The values on route a were between 36 °C and 37.5 °C, and the slight increase on route B reached 1.5 °C.

At 17:00, due to the sun's direction, a noticeable increase in DPET on route A reached 5 °C at the end of the walk. Route B was in the shade for most of the walk, and that helped to maintain a slight increase in the DPET, which reached 3.0 °C. On both routes, adding trees helped to keep the DPET values steady from beginning to end.

The results for Mohandisen are shown in Figure 11. At 9:00, route A showed a regular slight DPET increase until reaching 37.5 °C at the end of the walk, which was an increase of 4 °C. Route B increased significantly to reach 45 °C, an increase of 10.5 °C, at the end of the northeastern shallow canyon, then started to decrease while moving within the moderate northwestern canyon to reach 42.0 °C at the end. Adding trees to both routes helped route A maintain almost steady DPET values of 33 °C to 34 °C and helped route B reduce the massive increase in the DPET by 2.5 °C, as it started at DPET = 33.0 °C, reached a maximum value of 42.0 °C, and decreased to 38.0 °C at the end.

At 11:00, both routes started with very high DPET values. Route A decreased by 2.5 °C then increased again to end the walk with the same value. Route B increased to reach 52.5 °C at the end of the shallow northeastern canyon then decreased in the moderate northwestern canyon to reach 48.5 °C at the end. Increasing the tree density somewhat controlled the massive increase and the extreme heat stress values on both routes. On route A, the trees helped to reduce the high starting value by 3.0 °C to end the walk with DPET = 42.5 °C. On route B, the trees helped to avoid any increase in the DPET above 50.0 °C, as the maximum DPET value recorded at the end of the shallow northeastern canyon was 49.0 °C, which was 3.5 °C lower than in the scenario with lower tree density. Route B started at DPET = 46.0 °C, and the walk ended with a lower DPET value = 45.0 °C. T Skin fluctuation occurred at both 9:00 and 11:00 due to the massive heat stress and a lack of shading, which led to an increase of 1.5 °C in the skin temperature.

At 13:00, a very similar DPET performance was observed. The only difference was that both routes had higher DPET values at 13:00. Route A fluctuated slightly (within 2 °C) because of the impact of the moderate canyons and the urban park in the middle until reaching the same value as the starting point at the end. Route B had a very high DPET value at the beginning of the walk (50.5 °C) then increased to reach 54.0 °C at the end of the shallow northeastern canyon and decreased to reach the same value as the starting point at the end of the route. Increasing the tree density was crucial at this hour when the building's shade had almost vanished. On route A, it provided a good DPET reduction of 3 °C at the end of the route. On route B, it helped to keep the DPET under 50.0 °C for the whole route with a reduction of 1.5 °C at the end.

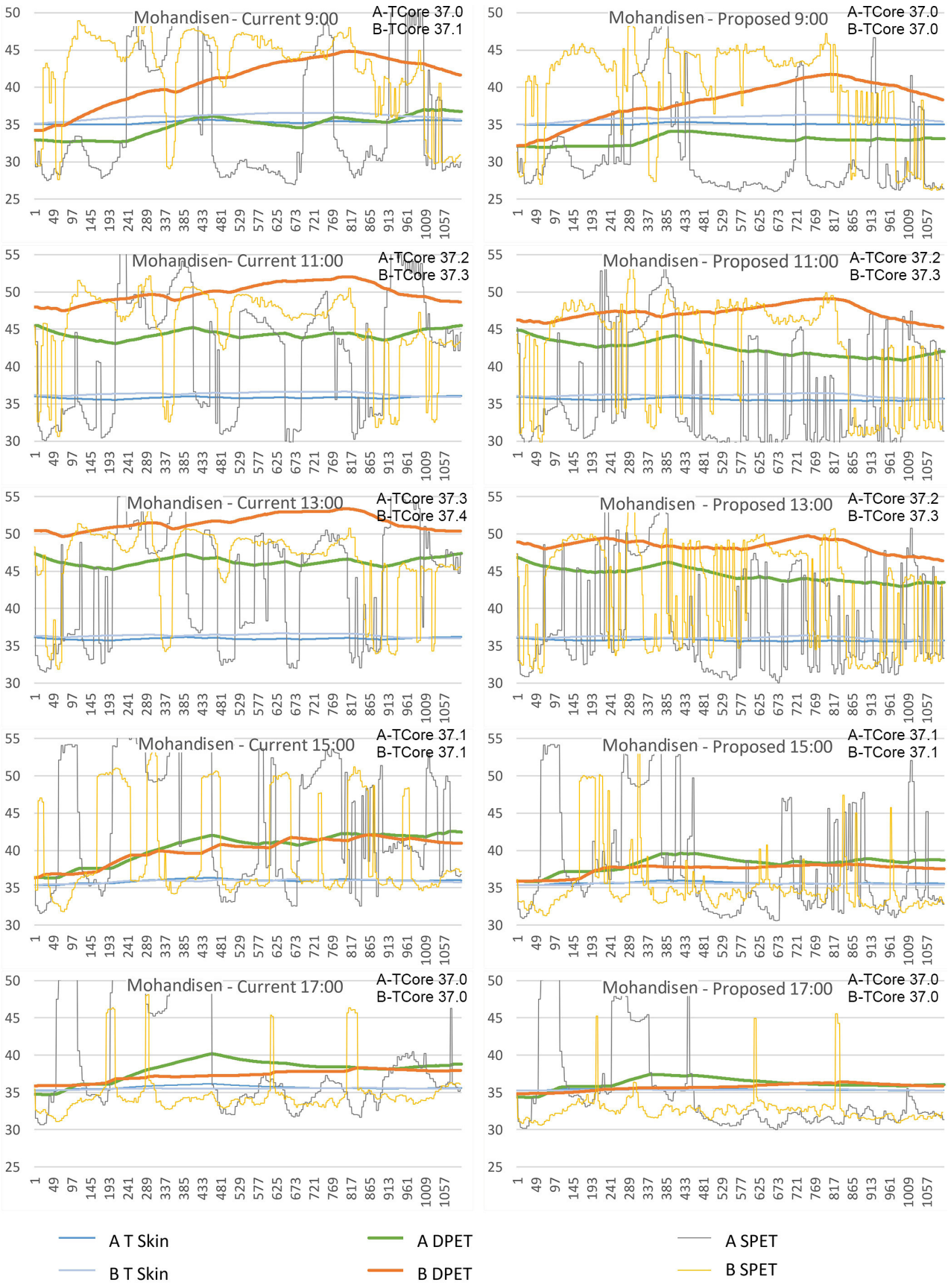



**Figure 11.** DPET, SPET, skin temperature (T Skin), and average core temperature (TCore) results for Mohandisen routes (A and B) in both tree scenarios (current and proposed) at Z = 1.5 m. Y axis = °C and X axis = seconds while walking each route.

At 15:00, when urban shading took place, the DPET values decreased significantly on both routes. Routes A and B both had slight regular increases in DPET of 7 °C at the end. Adding trees enhanced the performance more when tree shading was mixed with building shading, which limited the DPET increase to 3.0 °C to 4.0 °C on both routes. Here, the importance of urban shading when mixed with tree shading appeared for these moderate canyons at one of the peak hours (15:00).

At 17:00, the importance of urban shading appeared again, and it helped to keep the DPET values on both routes under 40.0 °C. On route A, the DPET was 35.0 °C at the starting point. It reached 40.0 °C before the urban park then decreased to 38.0 °C at the end. On route B, the DPET showed a regular slight increase of 1.5 °C at the end. Increasing the tree density on both routes helped to keep the DPET stable for the whole walk and within the range of the skin temperature.

In New Cairo, as shown in Figure 12, the good amounts of green open spaces (12%) and trees (9.4%) in the current situation helped to keep the DPET values lower. However, urban shading was very limited due to the lower heights of the buildings and the applied plot setbacks, and the impact of trees was essential to enhancing the thermal comfort of pedestrians. At 9:00, both routes had regular gradual increases that reached 8 °C at the end. Higher tree density helped to reduce these big increases. Route A showed a quick DPET increase of 4.5 °C while walking on the sidewalk then stayed steady until the end. Route B had a regular gradual increase of 4.5 °C.

At 11:00, both roads showed regular DPET increases that reached 9.0 °C at the end. Higher tree density helped to reduce the increases on both routes to only 4.5 °C, which was under the skin temperature. At 13:00, the same thermal performances took place with DPET values of 35.0 °C on both routes. Then, regular increases took place until reaching 43.0 °C at the ends of both routes for increases of 8.0 °C. In the scenario with increased tree density, the trees helped to reduce the increases to only 3.5 °C at the ends of both routes.

At 15:00, similar thermal conditions were observed with regular gradual increases of 9.0 °C on routes A and B. Then, the increase in tree density reduced the DPET increases significantly to only reach 2.5 °C at the ends of both routes. At 17:00, routes A and B had the same DPET value (34.0 °C) at the starting points. Then, the same increase happened, but it was lower than at the other hours, as it reached 5 °C, and both routes had values of 39.0 °C at the end. Increasing the tree density led to both routes maintaining very stable DPET values ranging between 34.0 °C and 35.0 °C from beginning to end.

The results in New Cairo showed the importance of trees in both scenarios (low tree density and high tree density). When the urban form is very open and urban shading has almost vanished, tree shading is a proper solution that can be used to enhance microclimate conditions. This case also showed that the surface material has a limited impact, as walking inside the park or on the sidewalk resulted in a slight performance change as long it occurred under the same tree's coverage.

In Mivida, as shown in Figure 13, similar DPET performances took place as the DPET mainly depended on the tree cover percentage due to the absence of building shading because the buildings were short (villas with G + 2) and because of the setbacks inside each plot, which set all buildings away from both the sidewalk and the walking trails inside the parks. At 9:00, route A had a higher DPET value. The good density of the trees inside the urban park helped to reduce the DPET, and both routes reached the same DPET value (34.0 °C) at the road crossings. Then, route A increased slightly by 1.5 °C at the end, and route B stayed almost the same until the end. Increasing the tree density, which occurred more inside the parks than on the streets, helped to keep route A cooler than route B by 2 °C, and increasing the number of trees led to both routes maintaining steady DPET performances, ranging between 29.0 °C and 32.5 °C.

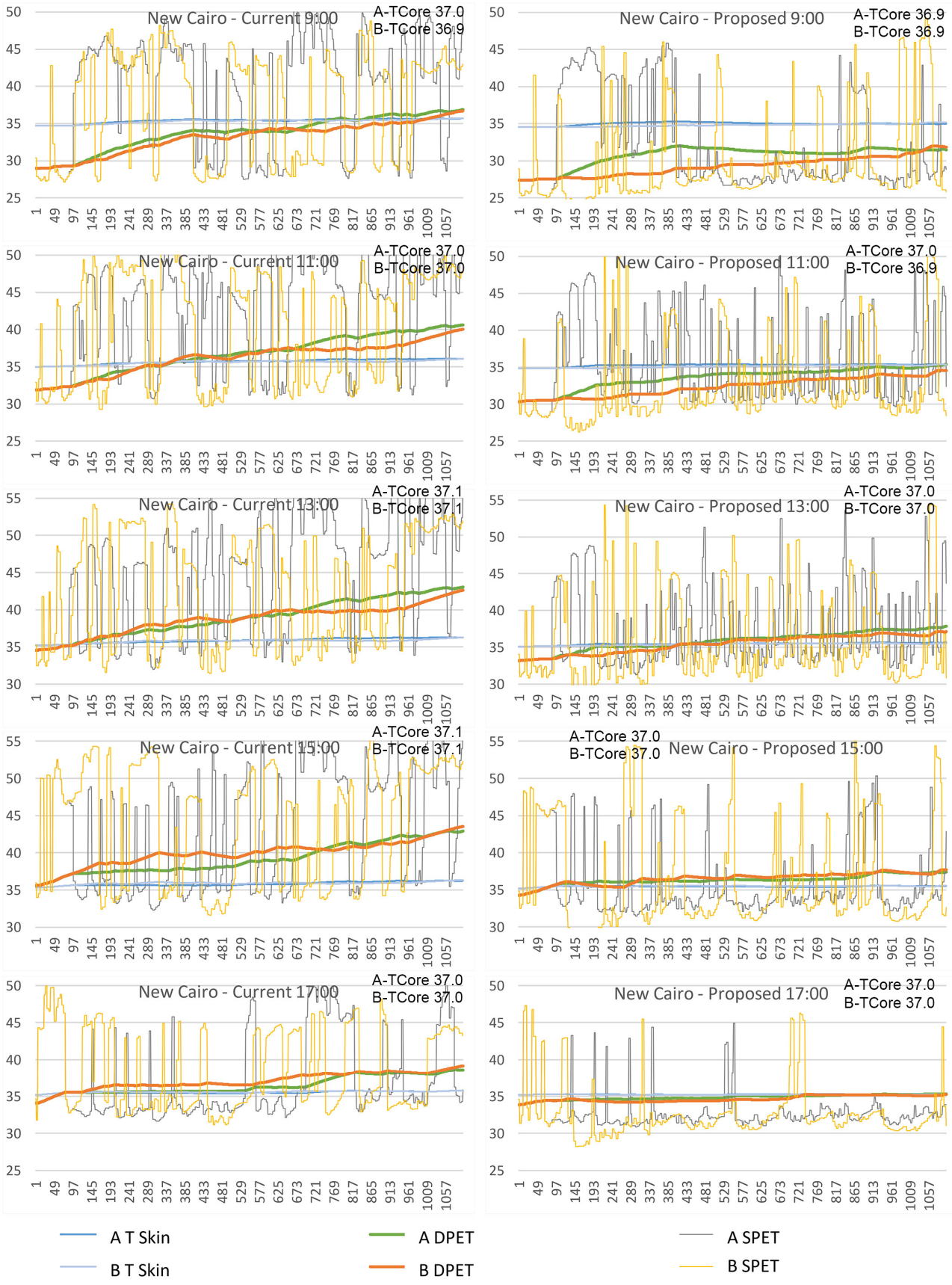



**Figure 12.** DPET, SPET, skin temperature (T Skin), and average core temperature (TCore) results for New Cairo routes (A and B) in both tree scenarios (current and proposed) at Z = 1.5 m. Y axis = °C and X axis = seconds while walking each route.

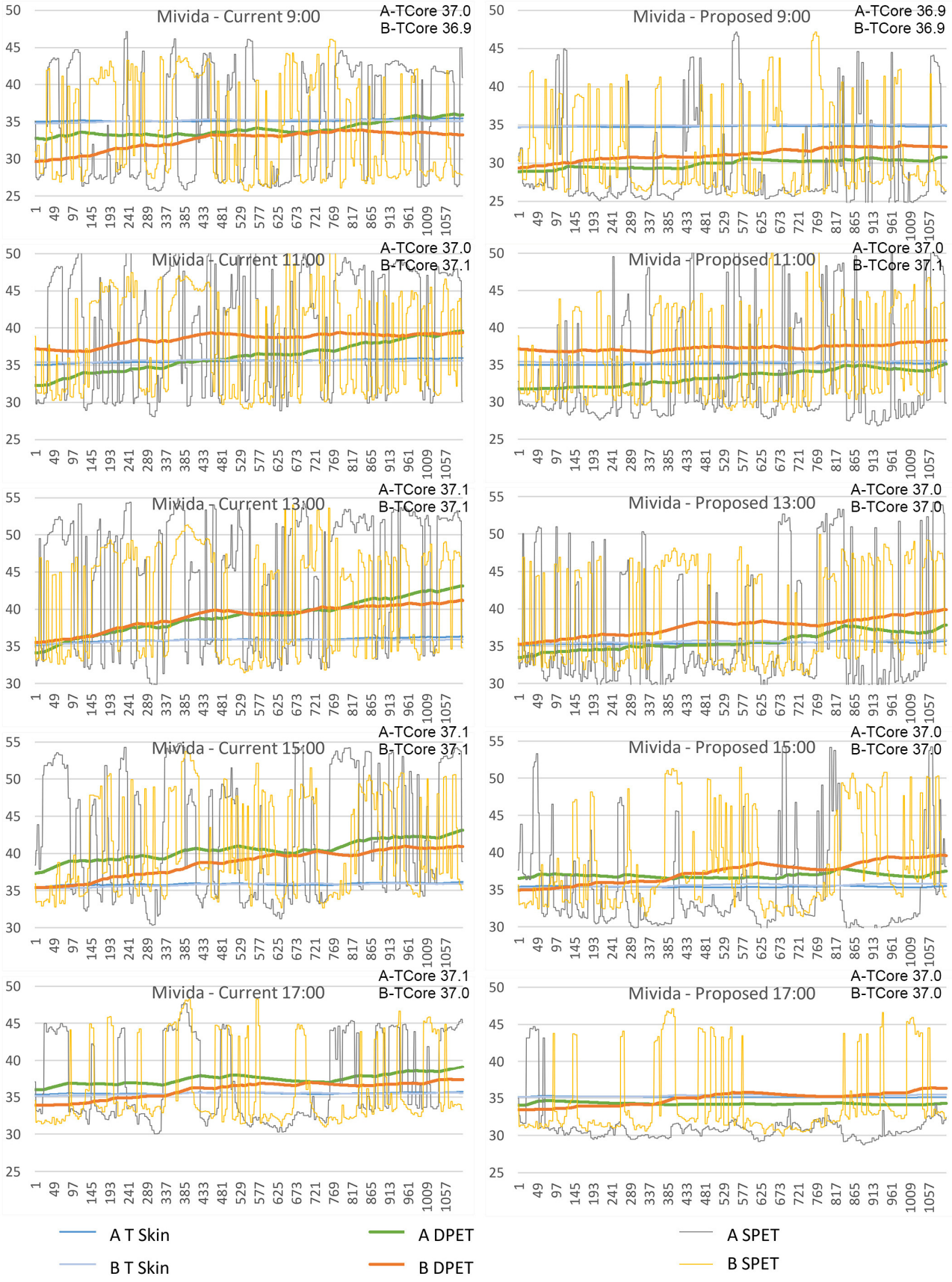



**Figure 13.** DPET, SPET, skin temperature (T Skin), and average core temperature (TCore) results for Mivida routes (A and B) in both tree scenarios (current and proposed) at Z = 1.5 m. Y axis = °C and X axis = seconds while walking each route.

At 11:00, route A had a good DPET value at the starting point (32.5 °C), which was lower than that of route B (37.5 °C). Then, route A had a larger DPET increase, and both routes reached the same value at the end of the walk (39.5 °C). This lower DPET increase on route B was due to the higher density of trees on the road in the current situation on this part of the route.

Increasing the tree density on both routes (the density was higher in parks) helped both routes to maintain lower DPET values, especially route A, which started and ended within the same range as the skin temperature. On route B, a slight increase in the tree density helped to keep the DPET value more stable within the range of 37.0 °C to 38.0 °C.

At 13:00, the DPET increased by 8.5 °C by the end of route A and by 6.5 °C by the end of route B. Increasing the tree density, especially in the parks, helped to keep route A cooler than route B by 2.0 °C to 3.0 °C and kept the whole walks on both routes under 40.0 °C.

At 15:00, route B was cooler than route A due to the impact of mixed shading from trees and buildings. Route A started with DPET = 37.0 °C then increased to reach 39.0 °C at the end of the route. Route B started with DPET = 34.0 °C then increased to reach 41.0 °C at the end of the route. Increasing the tree density totally changed the results. Route A was 2.0 °C cooler than route B at the end of the route. However, this route had a higher DPET value at the beginning (1 °C higher than route B).

At 17:00, additional building shading combined with tree shading helped to keep route B 1.5 °C to 2.0 °C cooler than route A for the whole walk. On the contrary, increasing the tree density in the parks helped to keep route A slightly cooler (1.0 °C). Increasing the tree density led to stable DPET values ranging between 34.0 °C and 34.5 °C on route A and in the range of 33.5 °C to 36.0 °C on route B.

In the Mohandisen study, the maximum core temperature and skin temperature were recorded, with an average core temperature of 37.4 °C on route B in the current Mohandisen scenario, which reflected how the climate conditions were harsh on this route at this hour (13:00). Similarly, the second highest average core temperature was recorded on route A in the current scenario at the same hour.

To conclude, the DPET changed between the different routes under the different tree scenarios. Table 7 shows the DPET values in the classified categories at the critical hours (13:00 and 15:00) every 50 s from the beginning until the end of each route. As shown in the table, routes A and B in Mohandisen and route B in Bulaq were the main critical routes that almost fell under the worst condition for the whole walks (red color range). However, in the tree scenarios, the DPET categories changed significantly, especially in the Bulaq cases. Other routes were in better conditions (the blue range) more often in the scenarios with increased trees.

### *3.3. Impact of SPET on DPET*

Based on the DPET results, it was clear that each point of thermal comfort (SPET) had an impact on the DPET. In some cases, when the SPET values were in a lower range than the DPET, the DPET curve decreased. On the contrary, when the SPET values were higher than the DPET, the DPET curve increased. DPET values that fluctuated in a very small range were not the same as the SPET. Therefore, controlling the SPET at each point will lead to control of the DPET, and for better DPET values, the SPET should be controlled for a larger part of the route. Thus, trees should be optimized to be integrated with building shading. As shown in the results, trees had different performances based on the urban form (aspect ratio and orientation) and based on the time of day and the location of the sun. Figure 14 shows SPET comparisons for each study area and both tree scenarios (proposed and current) for the two peak hours of daytime (13:00 and 15:00). It is very obvious that trees are quite important at noon, when building shading disappears, and trees are also important at 15:00 in cases when buildings do not provide enough shading to the urban canyon. This applies in New Cairo and Mivida, where SPET reductions around 16.0 °C were identified due to the absence of building shading. On the contrary, in a compacted urban form such as Bulaq, the majority of open spaces are green, as shown in the maps,

which proves that increasing tree density in such a compacted form will help to enhance the SPET values. However, this enhancement is not as significant as in open urban forms with higher sky view factors (SVFs) and more open spaces. These maps provide evidence that for moderate urban forms such as those in Downtown and Mohandisen, higher tree density is better, especially for wider canyons such as those in Mohandisen, which need more trees. As shown in the map, many urban canyons were still in the green category even after increasing the tree cover percentage. When increasing the tree density, the amount of building shading should be considered, as overlapping shading from buildings and trees will not enhance the SPET, as shown in the Downtown maps, especially at 15:00. This would be a waste of resources, especially for a country like Egypt that suffers from water scarcity [55].

**Table 7.** Main DPET value classifications (every 50 s) on all routes in all scenarios at the critical hours (13:00 and 15:00).

| Time | 13:00 | | | | | | | | | | | | 15:00 | | | | | | | |
|---|---|---|---|---|---|---|---|---|---|---|---|---|---|---|---|---|---|---|---|---|
| | A | | | | | B | | | | | A | | | | | B | | | | |
| | Downtown | Bulaq | Mohandisen | New Cairo | Mivida | Downtown | Bulaq | Mohandisen | New Cairo | Mivida | Downtown | Bulaq | Mohandisen | New Cairo | Mivida | Downtown | Bulaq | Mohandisen | New Cairo | Mivida |
| Current | | | | | | | | | | | | | | | | | | | | |
| 0 | 38 | 37 | 47 | 35 | 34 | 36 | 47 | 50 | 35 | 36 | 39 | 40 | 36 | 36 | 37 | 36 | 50 | 36 | 36 | 35 |
| 50 | 39 | 39 | 46 | 35 | 36 | 37 | 45 | 50 | 35 | 36 | 39 | 41 | 37 | 37 | 39 | 36 | 48 | 37 | 37 | 36 |
| 100 | 40 | 41 | 45 | 37 | 37 | 38 | 45 | 51 | 37 | 37 | 40 | 43 | 38 | 38 | 39 | 37 | 48 | 38 | 39 | 37 |
| 150 | 41 | 42 | 46 | 37 | 38 | 38 | 45 | 52 | 38 | 38 | 40 | 44 | 40 | 38 | 39 | 37 | 47 | 40 | 40 | 37 |
| 200 | 41 | 43 | 47 | 38 | 39 | 40 | 44 | 51 | 39 | 39 | 41 | 45 | 41 | 38 | 41 | 39 | 46 | 40 | 40 | 38 |
| 250 | 42 | 41 | 46 | 38 | 39 | 42 | 44 | 52 | 38 | 40 | 41 | 43 | 42 | 38 | 41 | 41 | 45 | 41 | 39 | 39 |
| 300 | 41 | 41 | 46 | 39 | 39 | 42 | 44 | 53 | 40 | 39 | 41 | 42 | 41 | 39 | 40 | 41 | 45 | 40 | 40 | 40 |
| 350 | 42 | 40 | 46 | 40 | 40 | 43 | 45 | 53 | 40 | 40 | 41 | 41 | 41 | 40 | 40 | 41 | 44 | 42 | 41 | 40 |
| 400 | 41 | 40 | 47 | 41 | 40 | 43 | 45 | 53 | 40 | 40 | 41 | 41 | 42 | 41 | 41 | 42 | 44 | 41 | 41 | 40 |
| 450 | 42 | 40 | 46 | 42 | 41 | 43 | 45 | 52 | 40 | 40 | 42 | 40 | 42 | 42 | 42 | 43 | 44 | 42 | 41 | 41 |
| 500 | 41 | 40 | 47 | 42 | 42 | 43 | 44 | 51 | 41 | 41 | 42 | 40 | 42 | 42 | 42 | 43 | 43 | 41 | 42 | 41 |
| Proposed | | | | | | | | | | | | | | | | | | | | |
| 0 | 36 | 36 | 47 | 33 | 34 | 35 | 45 | 49 | 33 | 35 | 36 | 38 | 36 | 34 | 37 | 35 | 47 | 36 | 34 | 35 |
| 50 | 36 | 37 | 45 | 34 | 34 | 36 | 43 | 48 | 34 | 36 | 36 | 38 | 37 | 36 | 37 | 36 | 46 | 36 | 36 | 35 |
| 100 | 36 | 38 | 45 | 35 | 35 | 37 | 43 | 49 | 34 | 36 | 36 | 38 | 37 | 36 | 37 | 36 | 45 | 37 | 36 | 36 |
| 150 | 37 | 38 | 45 | 35 | 35 | 37 | 42 | 49 | 35 | 37 | 37 | 38 | 38 | 36 | 37 | 36 | 44 | 38 | 36 | 36 |
| 200 | 37 | 39 | 46 | 35 | 35 | 37 | 41 | 48 | 35 | 37 | 37 | 39 | 39 | 36 | 36 | 37 | 43 | 38 | 36 | 37 |
| 250 | 37 | 38 | 45 | 36 | 35 | 38 | 40 | 48 | 35 | 38 | 37 | 38 | 39 | 36 | 37 | 38 | 42 | 38 | 37 | 37 |
| 300 | 37 | 37 | 44 | 36 | 36 | 39 | 40 | 48 | 36 | 38 | 37 | 37 | 39 | 36 | 37 | 37 | 41 | 38 | 37 | 38 |
| 350 | 37 | 37 | 44 | 37 | 36 | 38 | 40 | 49 | 36 | 38 | 37 | 37 | 38 | 36 | 37 | 38 | 41 | 38 | 37 | 38 |
| 400 | 37 | 36 | 44 | 37 | 37 | 39 | 39 | 49 | 37 | 38 | 37 | 37 | 38 | 36 | 37 | 38 | 40 | 38 | 37 | 38 |
| 450 | 37 | 36 | 43 | 37 | 37 | 39 | 39 | 48 | 37 | 39 | 37 | 36 | 39 | 37 | 37 | 38 | 40 | 38 | 37 | 39 |
| 500 | 37 | 36 | 43 | 37 | 37 | 39 | 39 | 47 | 37 | 39 | 36 | 36 | 38 | 37 | 37 | 38 | 40 | 38 | 37 | 39 |
| Scale | Better conditions | | | | | | | | | | | | | | | | Worse conditions | | | |

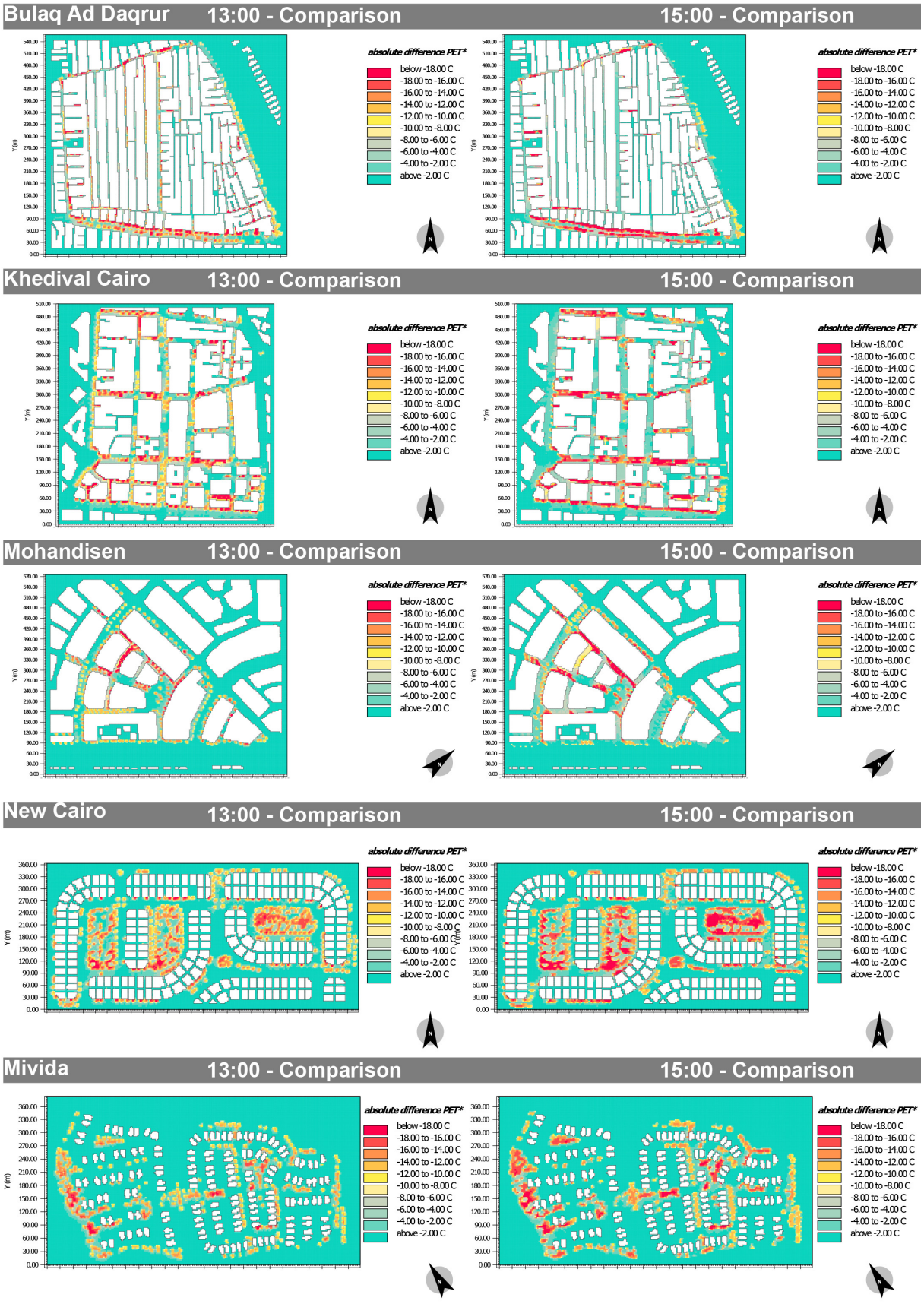



**Figure 14.** PET comparison (proposed vs. current) for all study areas at 13:00 and 15:00 at Z = 1.5 m.

### *3.4. Impact of Trees*

The impact of trees can be observed based on the varying results (significant in some areas and minor in others). Increasing the tree density plays an important role when canyons are wide, especially when they are oriented to the east. This is in line with [21,26,31,50]. Full comparisons were applied to all routes before and after increasing the tree density to understand how the impact of the trees changed between different routes in different areas. This analysis helped to decide which cases need more trees to optimize thermal comfort. A classification analysis was applied to each route by the second to show how trees helped to change the thermal comfort zone for pedestrians while walking. This analysis clarified how long each walk was in each thermal comfort category. The thermal comfort zones considered the following grades of physiological stress (PET): 23 to 29 °C, slight heat stress (slightly warm); 29 to 35 °C, moderate heat stress (warm); 35 to 41 °C, strong heat stress (hot); more than 41 °C, extreme heat stress (very hot) [56]. The value used for internal heat production was 80 W, and heat transfer from clothing was 0.9 clo [57]. As shown in Figure 15, routes in some study areas were under extreme heat stress. Especially during the peak hours (11:00, 13:00, and 15:00) in Mohandisen, most of the walks (90% or more) were under extreme heat stress on both routes, while better performances took place in both Downtown and Bulaq, as each route had a balance between strong and moderate heat stress zones during the peak hours. In New Cairo and Mivida, better performances were observed, as all routes were mostly located within the moderate heat stress zone with a very limited percentage under extreme heat stress. In all tree scenarios, significant changes took place and new classifications appeared (such as slightly warm). Most of the classifications were within the warm zone, with very limited presence of extreme heat stress, which only occurred on route B in Mohandisen due to a large shallow canyon. Increasing the tree density was more significant on both routes in New Cairo and Mivida, as most of the routes fell within the warm to hot categories. Almost the same results were observed in Downtown and Bulaq, with some slight changes in Bulaq due to the wide canyon at the start of the walk.

The findings of this study matched those of many other scholars. For example, the performance of the trees was closely related to the urban form. In Bulaq, when pedestrians were walking inside the deep northern canyon, the DPET was enhanced even without trees [21,58], while trees' significance was clear when the canyons were shallow and lacked shading [59–61]. Also, it was clear that increasing the tree density in areas that already had adequate tree percentages (such as in New Cairo and Mivida) helped to provide better dynamic thermal comfort [62]. Therefore, it is obvious that adding trees is important, but the urban form and urban characteristics should be considered to optimize the use of trees [21,50].

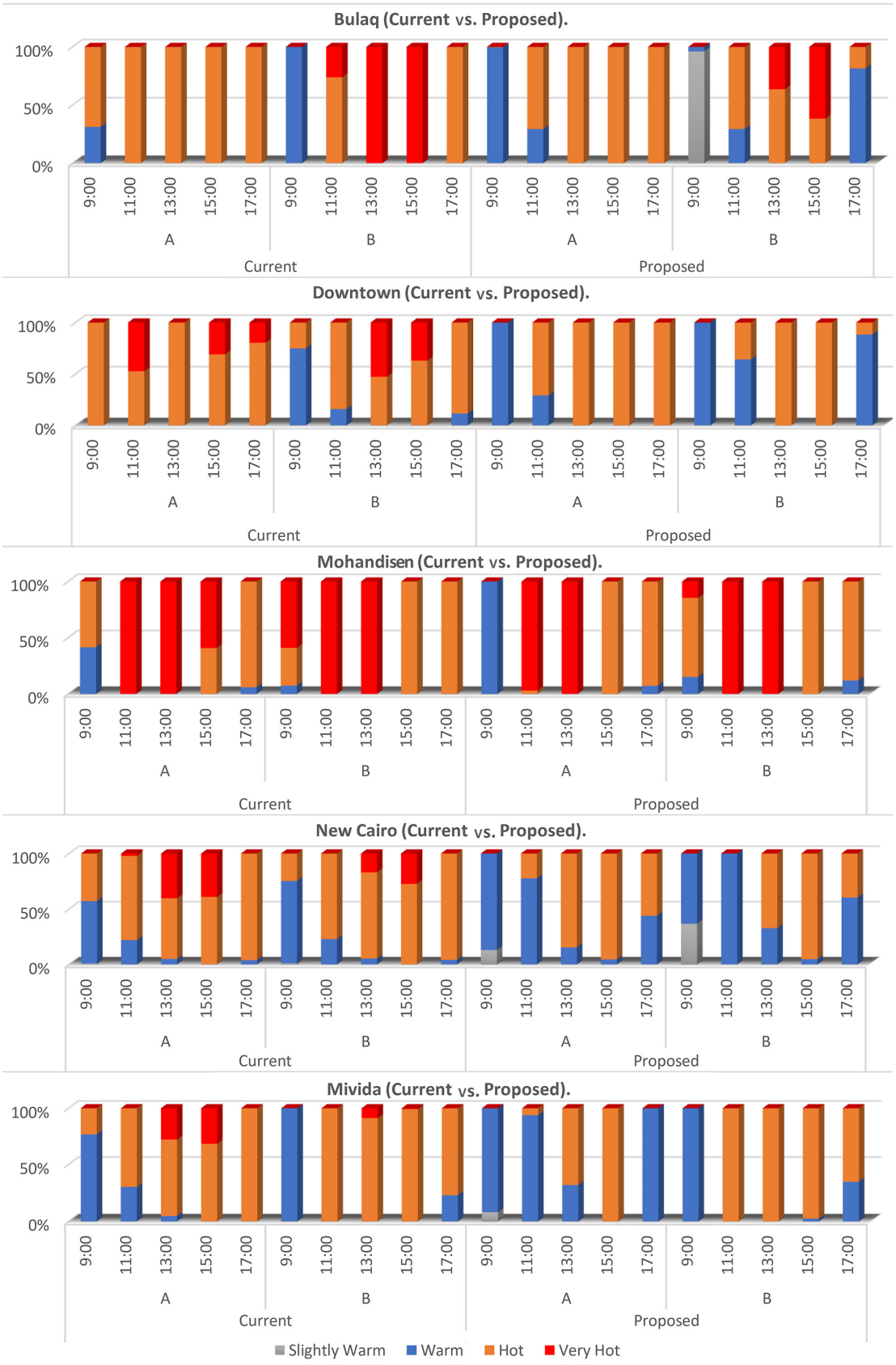



**Figure 15.** The dynamic thermal comfort classifications for each route (A and B) in both tree scenarios (current and proposed). The DPET values were exported at Z = 1.5. The X axis represents the hours, and the Y axis represents the percentages.

### *3.5. DPET Changes between Routes*

A more detailed analysis was conducted, and the DPET results of each route (A and B) in both tree scenarios were compared to understand how the impact of the urban form and urban trees could change the DPET significantly even within the same area. As shown in Figure 16, starting with Bulaq's current scenario, route B started with very high values at 13:00 and 15:00, with DPET values reaching 10 °C. Due to the better canyon aspect ratio, this difference decreased significantly to only 1.5 °C. Then, both routes had the same performance on the northern road until the end. For the other hours, route B showed better performances than route A, with DPET values that were 3 °C lower on average. In the proposed tree scenario in Bulaq, the same performances happened at the same hours. The only difference was a slightly better DPET value. In Downtown, route A had higher DPET values at the starting point, with an average of 3.5 °C for all hours. However, the better canyon orientation helped to reduce this higher starting point, especially during the peak hours (13:00 and 15:00) and made route A better than route B by an average of 1 °C during the last part of the walk in the current scenario. In the proposed scenario, the trees controlled the DPET increase, especially at the starting point, and limited the changes to only 1 °C higher values at the beginning of route A and 1 °C lower values at the end of route A at almost all hours. In Mohandisen, however, routes A and B had the same DPET at the starting point. Due to the harsh climate conditions on route B, the difference in the DPET increased enormously and reached an average of 8 to 9 °C at three times (9:00, 11:00, and 13:00). A limited increase in trees did not help much, as the same performance, with an average DPET value of 2 °C, took place, which was an indicator that trees should be increased more in this study area. In New Cairo, routes A and B had slight DPET differences ranging between 1 °C and −1 °C. Route A was higher at the beginning. Then, route B became higher at most of the hours in the current scenario. In the proposed tree scenario, due to the increase in trees in the urban parks, route B became cooler for the whole walk and route A reached a DPET up to 2.5 °C higher during the first half of the walk before decreasing to 1 °C higher at the end of the walk. In Mivida, very similar performances took place. Route A (passing by the green parks) was higher due to the limited trees in the current scenario and reached an average of 2 °C higher after the various starting DPET values, except for at 11:00, when the DPET decreased from 5 °C higher to reach 0 and the end. In the trees scenario, the performances were reversed. Route A became cooler for the whole walk due to the greater increase in trees inside the parks than along the roads and reached an average of 2 °C cooler at most of the times. This proved that thermal comfort was mainly driven by the local microclimate conditions of a canyon or a space, and the overall study area did not control the thermal comfort of pedestrians.

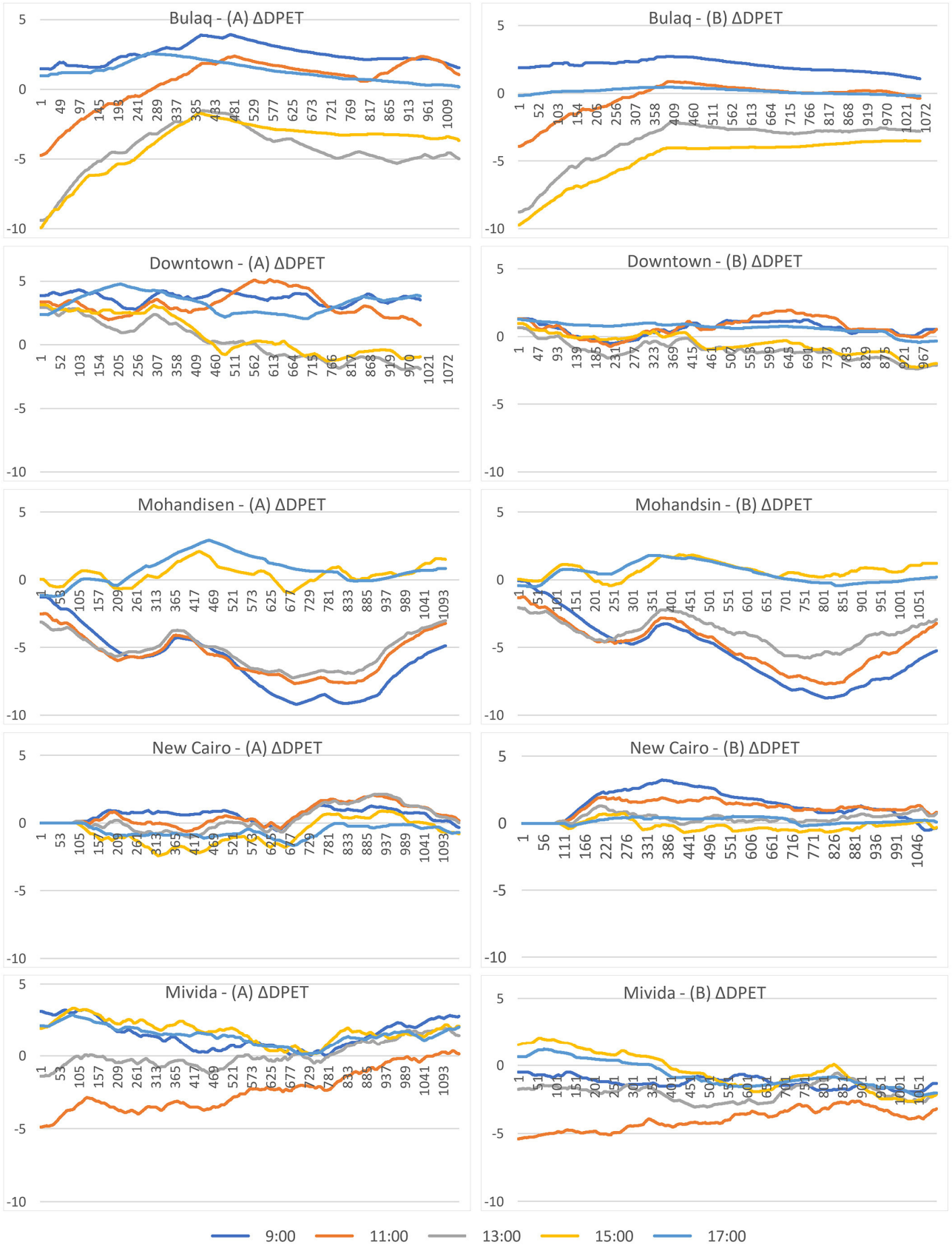



**Figure 16.** The Δ DPET in each study area. A represents (A–B) in the current situation, and B represents (A–B) in the proposed situation at Z = 1.5 m. The Y axis represents the ΔDPET (°C), and the X axis represents the time of the walk (seconds).

## 4. Discussion

The various results were driven by changes in the urban forms (aspect ratios and orientations) and tree densities, which was in line with [12,21,24,27,50]. More analyses were applied to have a full understanding of the effect of each factor. This included a detailed study of the changes between the different study areas.

*DPET Changes between Different Study Areas*

The changes between the hotter routes in each study area were analyzed to understand the range of differences not only in each area but also between them. The DPET values of route (A) in Bulaq, route (B) in Mohandisen, route (A) in New Cairo, and route (B) in Mivida were compared to route (B) in Downtown, as shown in Figure 17. At 9:00, all study areas except Mohandisen had a similar DPET range of 33 °C to 37 °C for the majority of the walks. Higher values were mainly observed in Bulaq, but route B in Mohandisen showed a significant DPET increase that reached 10 °C. Adding trees helped to keep the DPET range between 29 °C and 32 °C at the ends of the walks for all routes except route B in Mohandisen, where the higher range was reduced by 2 °C on average. At 11:00, the same performances took place, and all routes had similar DPET values of around 39.5 °C. However, most of them had different DPET values at the starting points. The only difference was for route B in Mohandisen, which still showed significantly higher DPET values with an average of 50 °C in the current situation. This was 10 °C higher than on route B in Downtown. Adding trees led to better DPET values around 36 °C at the ends of the walks for all routes, except for route B in Mohandisen, where the DPET value improved slightly to around 47 °C. At 13:00, the same performances took place. The difference in DPET on route B in Mohandisen was a range of 10 °C, and route A in Bulaq had slight DPET changes of around 3.0 °C. Increasing the tree density reduced this range to 1 °C and improved the condition on route B in Mohandisen by 1 °C. At 15:00 and 17:00, due to good shading by buildings, the increase on route B in Mohandisen decreased significantly, and the DPET values were within the same ranges for all routes (below 38 °C in the current scenario and 35 °C in the proposed tree scenario). This is also proof that the DPET was driven by the microclimate conditions of the canyons more than the overall urban context, and changes between different urban canyons could sometimes reach 10 °C.

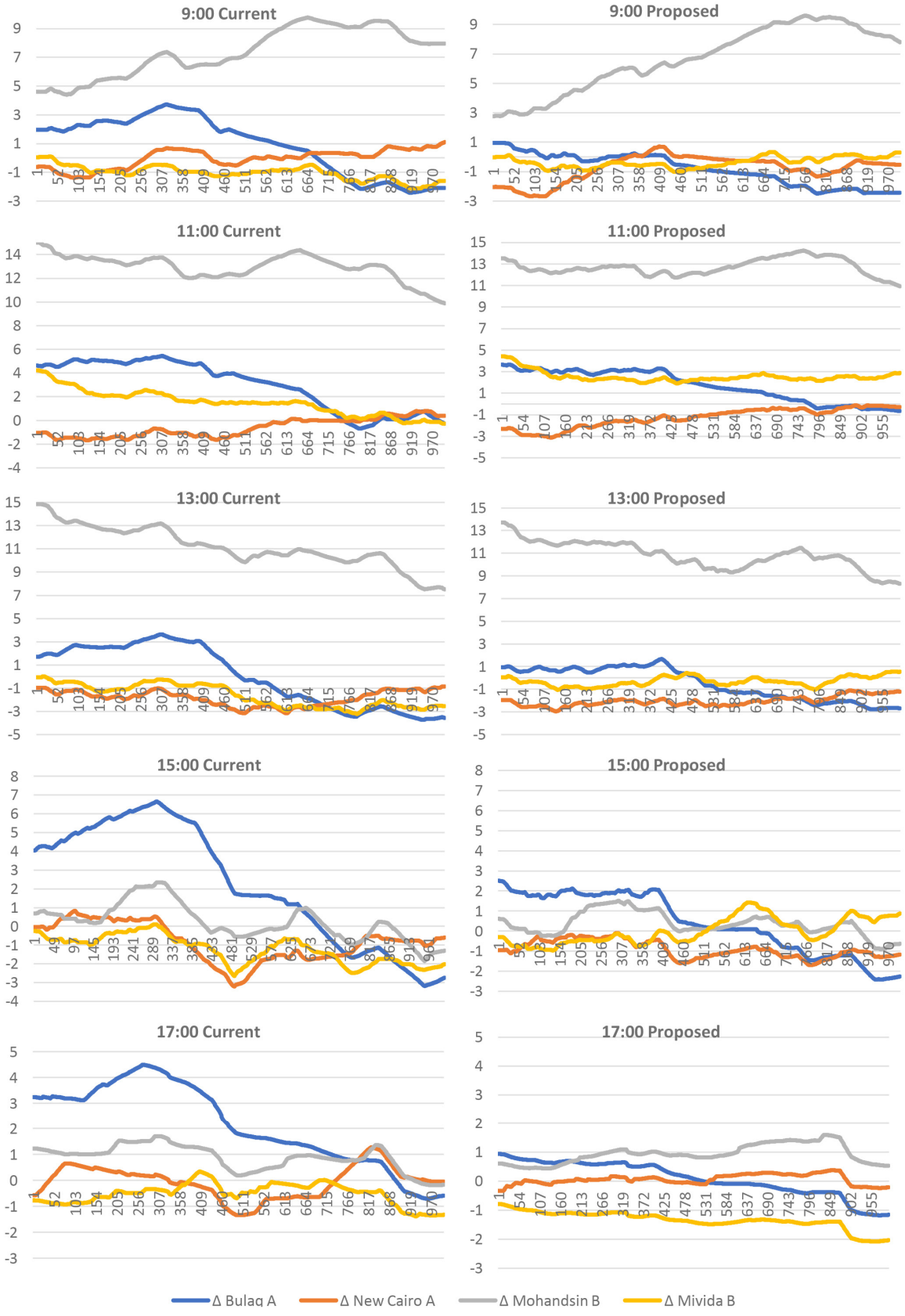



**Figure 17.** The ΔDPET values on the hot routes in each study area compared to route B in Downtown for the current and proposed scenarios at each hour at Z = 1.5 m. The Y axis represents the DPET (°C), and the X axis represents the time of the walk (seconds).

## 5. Conclusions

The parameters currently used to measure thermal comfort, such as the steady/static thermal comfort (SPET), are not sufficient to represent real pedestrian thermal comfort while walking because they do not consider changes and dynamic variations in the thermal environment [1]. This study aimed to enhance the dynamic thermal comfort (DPET) of pedestrians while walking under different urban forms with different aspect ratios, orientations, building density, and trees density under the same climate data for all cases. After assessing five different study areas in Cairo City under two tree scenarios (the current tree density and a proposed increase in tree density), the results proved that the DPET had different values than the SPET at each point along the routes. However, the DPET was closely related to changes in the SPET. The main study findings can be summarized as follows:

- As the DPET was impacted by the SPET, keeping the SPET lower or higher for a long time reduced or increased the DPET.
- Frequent equivalent changes (ups and downs) in the SPET kept the DPET stable.
- Changes between DPET values were driven more by the microclimate conditions of a space or canyon than the conditions of the overall area, and controlling the microclimate conditions of a whole urban canyon controlled the DPET.
- Changes in the DPET could reach 10 °C between different canyons, and increasing the tree density could lower the DPET by up to 6 °C in some cases.

The DPET is affected more by urban shading (by buildings or trees) and wind than by changing paving materials or adding grass surfaces.

This study covered many urban forms and tree varieties and tested them using the simulation software ENVI-met V5.6.1, Winter 2023. It could also be linked to a real experiment by investigating how people walking on these routes are feeling. In addition, more urban routes could be studied, including different urban cases such as waterfront promenades, large-scale park walkways, or walkways inside large parking areas. The study outcomes should support design decisions like positioning bus stops in relation to the surrounding land use and walking conditions as well as the allocation of retail and commercial uses on routes and the allocation of urban parks and their frequency, which would not only be defined by the urban situation but also by studying thermal comfort.

**Author Contributions:** Conceptualization, A.Y.A.; Methodology, A.Y.A.; Software, A.Y.A.; Formal analysis, A.Y.A.; Writing—original draft, A.Y.A.; Writing—review & editing, D.G.; Visualization, A.Y.A.; Supervision, D.G. All authors have read and agreed to the published version of the manuscript.

**Funding:** This research did not receive any funding. APC was funded by TU Dortmund University.

**Data Availability Statement:** The data that support the findings of this study (all ENVI-met files) are available upon request.

**Conflicts of Interest:** The authors declare no conflicts of interest.

## Abbreviations

| | |
|---|---|
| UHI | urban heat island |
| SPET | (steady/static) physiological equivalent temperature |
| DPET | (dynamic) physiological equivalent temperature |
| TMRT | the mean radiant temperature |
| RH% | relative humidity |
| T Skin | skin temperature |
| T Core | core temperature |
| RMSE | root-mean-square error |
| d | index of agreement |
| SVF | sky view factor |

## References


1. Hwang, R.-L.; Weng, Y.-T.; Huang, K.-T. Considering transient UTCI and thermal discomfort footprint simultaneously to develop dynamic thermal comfort models for pedestrians in a hot-and-humid climate. *Build. Environ.* **2022**, *222*, 109410. [CrossRef]
2. Sauter, D. Measuring Walking: Towards internationally standardised monitoring methods of walking and public space. In Proceedings of the 8th International Conference on Survey Methods in Transport, Annecy, France, 25–31 May 2008.
3. Carolina, V.; Nikolopoulou, M. Thermal walks: Identifying pedestrian thermal comfort variations in the urban continuum of historic city centres. In Proceeding of PLEA2013-29th Conference, Sustainable architecture for a renewable futu. In Proceedings of the PLEA2013-29th Conference, Sustainable Architecture for a Renewable Future, Munich, Germany, 10–12 September 2013.
4. Carolina, V.; Nikolopoulou, M. Outdoor thermal comfort for pedestrians in movement: Thermal walks in complex urban morphology. *Int. J. Biometeorol.* **2020**, *64*, 277–291.
5. Richard, J.D.D.; Brager, G.S. Thermal comfort in naturally ventilated buildings: Revisions to ASHRAE Standard 55. *Energy Build.* **2002**, *34*, 549–561.
6. Fang, Y.; Chen, G.; Bicka, M.; Chen, J. Smart textiles for personalized thermoregulation. *Chem. Soc. Rev.* **2021**, *50*, 9357–9374. [CrossRef] [PubMed]
7. Zhai, H.; Fan, D.; Li, Q. Dynamic radiation regulations for thermal comfort. *Nano Energy* **2022**, *100*, 107435. [CrossRef]
8. Taleghani, M.; Kleerekoper, L.; Tenpierik, M.; van den Dobbelsteen Taleghani, A. Outdoor thermal comfort within five different urban forms in the Netherlands. *Build. Environ.* **2015**, *83*, 65–78. [CrossRef]
9. Li, J.; Niu, J.; Huang, T.; Mak, C.M. Dynamic effects of frequent step changes in outdoor microclimate environments on thermal sensation and dissatisfaction of pedestrian during summer. *Sustain. Cities Soc.* **2022**, *79*, 103670. [CrossRef]
10. Huang, T.; Niu, J.; Xie, Y.; Li, J.; Mak, C.M. Assessment of "lift-up" design's impact on thermal perceptions in the transition process from indoor to outdoor. *Sustain. Cities Soc.* **2020**, *56*, 102081. [CrossRef]
11. Katavoutas, G.; Flocas, H.A.; Matzarakis, A. Dynamic modeling of human thermal comfort after the transition from an indoor to an outdoor hot environment. *Int. J. Biometeorol.* **2015**, *59*, 205–216. [CrossRef]
12. Lau, K.K.-L.; Shi, Y.; Ng, E.Y.-Y. Dynamic response of pedestrian thermal comfort under outdoor transient conditions. *Int. J. Biometeorol.* **2019**, *63*, 979–989. [CrossRef]
13. Nakayoshi, M.; Kanda, M.; Shi, R.; de Dear, R. Outdoor thermal physiology along human pathways: A study using a wearable measurement system. *Int. J. Biometeorol.* **2015**, *59*, 503–515. [CrossRef] [PubMed]
14. Jia, X.; Cao, B.; Zhu, Y. A climate chamber study on subjective and physiological responses of airport passengers from walking to a sedentary status in summer. *Build. Environ.* **2022**, *207*, 108547. [CrossRef]
15. Höppe, P. Different aspects of assessing indoor and outdoor thermal comfort. *Energy Build.* **2002**, *34*, 661–665. [CrossRef]
16. Zhang, Y.; Liu, J.; Zheng, Z.; Fang, Z.; Zhang, X.; Gao, Y.; Xie, Y. Analysis of thermal comfort during movement in a semi-open transition space. *Energy Build.* **2020**, *225*, 110312. [CrossRef]
17. Theeuwes, N.E.; Steeneveld, G.J.; Ronda, R.J.; Heusinkveld, B.G.; van Hove, L.W.A.; Holtslag, A.A.M. Seasonal dependence of the urban heat island on the street canyon aspect ratio. *Q. J. R. Meteorol. Soc.* **2014**, *140*, 2197–2210. [CrossRef]
18. Theeuwes, N.E.; Steeneveld, G.J.; Ronda, R.J.; Heusinkveld, B.G.; van Hove, L.W.A.; Holtslag, A.A.M. Influence of aspect ratio and orientation on large courtyard thermal conditions in the historical centre of Camagüey-Cuba. *Renew. Energy* **2018**, *125*, 840–856.
19. Morakinyo, T.E.; Kong, L.; Lau, K.K.-L.; Yuan, C.; Ng, E. A study on the impact of shadow-cast and tree species on in-canyon and neighborhood's thermal comfort. *Build. Environ.* **2017**, *115*, 1–17. [CrossRef]
20. Ketterer, C.; Matzarakis, A. Human-biometeorological assessment of heat stress reduction by replanning measures in Stuttgart, Germany. *Landsc. Urban Plan.* **2014**, *122*, 78–88. [CrossRef]
21. Abdelmejeed, A.Y.; Gruehn, D. Optimization of Microclimate Conditions Considering Urban Morphology and Trees Using ENVI-Met: A Case Study of Cairo City. *Land* **2023**, *12*, 2145. [CrossRef]
22. Elsadek, M.; Liu, B.; Lian, Z.; Xie, J. The influence of urban roadside trees and their physical environment on stress relief measures: A field experiment in Shanghai. *Urban For. Urban Green.* **2019**, *42*, 51–60. [CrossRef]
23. Emmanuel, R.; Rosenlund, H.; Johansson, E. Urban shading—A design option for the tropics? A study in Colombo, Sri Lanka. *Int. J. Climatol. J. R. Meteorol. Soc.* **2007**, *27*, 1995–2004. [CrossRef]
24. Lobaccaro, G.; Acero, J.A.; Martinez, G.S.; Padro, A.; Laburu, T.; Fernandez, G. Effects of orientations, aspect ratios, pavement materials and vegetation elements on thermal stress inside typical urban canyons. *Int. J. Environ. Res. Public Health* **2019**, *16*, 3574. [CrossRef] [PubMed]
25. Shishegar, N. Street Design and Urban Microclimate: Analyzing the Effects of Street Geometry and Orientation on Airflow and Solar Access in Urban Canyons. *J. Clean Energy Technol.* **2013**, *1*, 52. [CrossRef]
26. De, B.; Mukherjee, M. Optimisation of canyon orientation and aspect ratio in warm-humid climate: Case of Rajarhat Newtown, India. *Urban Clim.* **2018**, *24*, 887–920. [CrossRef]
27. Aboelata, A. Vegetation in different street orientations of aspect ratio (H/W 1: 1) to mitigate UHI and reduce buildings' energy in arid climate. *Build. Environ.* **2020**, *172*, 106712. [CrossRef]
28. Wang, Y.; Berardi, U.; Akbari, H. Comparing the effects of urban heat island mitigation strategies for Toronto, Canada. *Energy Build.* **2016**, *114*, 2–19. [CrossRef]

29. Song, C.; Ikei, H.; Igarashi, M.; Miwa, M.; Takagaki, M.; Miyazaki, Y. Physiological and psychological responses of young males during spring-time walks in urban parks. *J. Physiol. Anthropol.* **2014**, *33*, 1–7. [CrossRef]
30. Takayama, N.; Korpela, K.; Lee, J.; Morikawa, T.; Tsunetsugu, Y.; Park, B.-J.; Li, Q.; Tyrväinen, L.; Miyazaki, Y.; Kagawa, T. Emotional, restorative and vitalizing effects of forest and urban environments at four sites in Japan. *Int. J. Environ. Res. Public Health* **2014**, *11*, 7207–7230. [CrossRef]
31. Abdollahzadeh, N.; Biloria, N. Outdoor thermal comfort: Analyzing the impact of urban configurations on the thermal performance of street canyons in the humid subtropical climate of Sydney. *Front. Archit. Res.* **2021**, *10*, 394–409. [CrossRef]
32. Andreou, E. Thermal comfort in outdoor spaces and urban canyon microclimate. *Renew. Energy* **2013**, *55*, 182–188. [CrossRef]
33. Jamei, E.; Ossen, D.R.; Seyedmahmoudian, M.; Sandanayake, M.; Stojcevski, A.; Horan, B. Urban design parameters for heat mitigation in tropics. *Renew. Sustain. Energy Rev.* **2020**, *134*, 110362. [CrossRef]
34. Envi-Board, Envi-Met Support Center. Envi-Met. Available online: http://www.envi-hq.com/ (accessed on 30 April 2023).
35. Kottek, M.; Grieser, J.; Beck, C.; Rudolf, B.; Rubel, F. World map of the Köppen-Geiger climate classification updated. *Meteorol. Z.* **2006**, *15*, 259–263. [CrossRef] [PubMed]
36. Abutaleb, K.; Ngie, A.; Darwish, A.; Ahmed, M.; Arafat, S.; Ahmed, F. Assessment of urban heat island using remotely sensed imagery over Greater Cairo, Egypt. *Adv. Remote Sens.* **2015**, *35*, 4. [CrossRef]
37. Panagiotis Kosmopoulos, H.E.-A.S.K. *The Solar Atlas of Egypt, Cairo: The EUMETSAT Network of Sataliete Application Facilities*; EUMETSAT: Darmstadt, Germany, 2018.
38. Climate Top. Available online: https://www.climate.top/egypt/cairo/temperatures/ (accessed on 1 June 2024).
39. Shahraiyni, H.T.; Sodoudi, S.; El-Zafarany, A.; El Seoud, T.A.; Ashraf, H.; Krone, K. A comprehensive statistical study on daytime surface urban heat island during summer in urban areas, case study: Cairo and its new towns. *Remote Sens.* **2016**, *8*, 643. [CrossRef]
40. Islam, A.E.-M.; Ismail, A.; Zanaty, N. Spatial variability of urban heat islands in Cairo City, Egypt using time series of Landsat Satellite images. *Int. J. Adv. Remote Sens. GIS* **2016**, *5*, 1618–1638.
41. Mohamed, E. Analysis of urban growth at Cairo, Egypt using remote sensing and GIS. *Nat. Sci.* **2012**, *4*, 355–361.
42. Eman, Z.; Vialard, A. Syntactic Stitching: Towards a Better Integration of Cairo's Urban Fabric. In *Proceedings of the 11th International Space Syntax Symposium*; Instituto Superior Técnico: Lisbon, Portugal, 2017.
43. Abougendia, S.M. Investigating surface UHI using local climate zones (LCZs), the case study of Cairo's River Islands. *Alex. Eng. J.* **2023**, *77*, 293–307. [CrossRef]
44. Elmarakby, E.; Khalifa, M.; Elshater, A.; Afifi, S. Spatial morphology and urban heat island: Comparative case studies. In *Architecture and Urbanism: A Smart Outlook: Proceedings of the 3rd International Conference on Architecture and Urban Planning, Cairo, Egypt*; Springer International Publishing: Cham, Switzerland, 2020; pp. 441–454.
45. Elbardisy, W.M.; Salheen, M.A.; Fahmy, M. Solar irradiance reduction using optimized green infrastructure in arid hot regions: A case study in el-nozha district, Cairo, Egypt. *Sustainability* **2021**, *13*, 9617. [CrossRef]
46. Zhang, J.; Gou, Z.; Zhang, F.; Yu, R. The tree cooling pond effect and its influential factors: A pilot study in Gold Coast, Australia. *Nat.-Based Solut.* **2023**, *3*, 100058. [CrossRef]
47. Liu, Y.; Lai, Y.; Jiang, L.; Cheng, B.; Tan, X.; Zeng, F.; Liang, S.; Xiao, A.; Shang, X. A study of the thermal comfort in urban mountain parks and its physical influencing factors. *J. Therm. Biol.* **2023**, *118*, 103726. [CrossRef]
48. Middel, A.; Chhetri, N.; Quay, R. Urban forestry and cool roofs: Assessment of heat mitigation strategies in Phoenix residential neighborhoods. *Urban For. Urban Green.* **2015**, *14*, 178–186. [CrossRef]
49. Shahidan, M.F.; Shariff, M.K.M.; Jones, P.; Salleh, E.; Abdullah, A.M. A comparison of Mesua ferrea L. and Hura crepitans L. for shade creation and radiation modification in improving thermal comfort. *Landsc. Urban Plan.* **2010**, *97*, 168–181. [CrossRef]
50. Abdelmejeed, A.G.D. Optimizing an efficient urban tree strategy to improve microclimate conditions while considering water scarcity: A case study of Cairo. *Discov. Sustain.* **2024**, *5*, 66. [CrossRef]
51. Elnabawi, M.; Hamza, N.; Dudek, S. Outdoor thermal comfort in the old Fatimid city, Cairo, Egypt. In *International Conference on "Changing Cities": Spatial, Morphological, Formal & Socio-Economic Dimensions*; Newcastle University: Newcastle, UK, 2013.
52. Weather and Climate. Available online: https://weather-and-climate.com/Cairo-July-averages (accessed on 31 October 2023).
53. Time and Date. Available online: https://www.timeanddate.com/weather/egypt/cairo/historic?month=7&year=2022 (accessed on 30 October 2023).
54. Xiao, J.; Yuizono, T. Climate-adaptive landscape design: Microclimate and thermal comfort regulation of station square in the Hokuriku Region, Japan. *Build. Environ.* **2022**, *212*, 108813. [CrossRef]
55. Osman, R.; Ferrari, E.; McDonald, S. Water scarcity and irrigation efficiency in Egypt. *Water Econ. Policy* **2016**, *2*, 1650009. [CrossRef]
56. Ballinas, M.; Morales-Santiago, S.I.; Barradas, V.L.; Lira, A.; Oliva-Salinas, G. Is PET an adequate index to determine human thermal comfort in Mexico City? *Sustainability* **2022**, *14*, 12539. [CrossRef]
57. Heaviside, C.; Macintyre, H.; Vardoulakis, S. The urban heat island: Implications for health in a changing environment. *Curr. Environ. Health Rep.* **2017**, *4*, 296–305. [CrossRef]
58. Sanusi, R.; Johnstone, D.; May, P.; Livesley, S.J. Street orientation and side of the street greatly influence the microclimatic benefits street trees can provide in summer. *J. Environ. Qual.* **2016**, *45*, 167–174. [CrossRef]

59. Hassan, A.; Tao, J.; Li, G.; Jiang, M.; Aii, L.; Zhihui, J.; Zongfang, L.; Qibing, C. Effects of walking in bamboo forest and city environments on brainwave activity in young adults. *Evid. Based Complement. Altern. Med.* **2018**, *2018*, 9653857. [CrossRef]
60. Wei, D.; Liu, B. The analysis and evaluation of thermal comfort at Shanghai knowledge & innovation community square. *Chin. Landsc. Archit.* **2018**, *34*, 5–12.
61. Liu, B.Y.; Mei, Y.; Kuang, W. Experimental research on correlation between microclimate element and human behavior and perception of residential landscape space in Shanghai. *Landsc. Arch.* **2016**, *32*, 5–9.
62. Ochiai, H.; Ikei, H.; Song, C.; Kobayashi, M.; Miura, T.; Kagawa, T.; Li, Q.; Kumeda, S.; Imai, M.; Miyazaki, Y. Physiological and psychological effects of a forest therapy program on middle-aged females. *Int. J. Environ. Res. Public Health* **2015**, *12*, 15222–15232. [CrossRef]

**Disclaimer/Publisher's Note:** The statements, opinions and data contained in all publications are solely those of the individual author(s) and contributor(s) and not of MDPI and/or the editor(s). MDPI and/or the editor(s) disclaim responsibility for any injury to people or property resulting from any ideas, methods, instructions or products referred to in the content.